SENCKENBERG

ORIGINAL PAPER

Molecular phylogeny and morphological comparison of the deep-sea genus *Alloptilella* Li, Zhan & Xu, 2021 (Octocorallia, Pennatulacea)

Pablo J. López-González[1] (ID)

Abstract

A previously described species and a new one belonging to the recently described sea pen genus *Alloptilella* Li, Zhan & Xu, 2021, are here described and illustrated based on a morphological and molecular study of materials collected in the Tasman Sea (SW Pacific) and at Puerto Rico (Caribbean Sea), respectively. The species, *Alloptilella moseleyi* comb. nov. (Kölliker, 1880) and *Alloptilella williamsi* sp. nov., are in overall agreement with the generic diagnosis of *Alloptilella*., based on the type species, *Alloptilella splendida* Li, Zhan & Xu, 2021. A single relatively large colony (55 to 95 cm in total length) is known for each of the three *Alloptilella* species. The transferred and the new species differ from the type species in having an opposite, rather than alternate, placement of polyp leaves along the rachis, colouration of autozooids, and mesozooids (in the case of *A. moseleyi* comb. nov.), and spicular features (e.g. maximum sizes in different parts of the colony, presence/absence of tentacular sclerites). *Alloptilella williamsi* sp. nov. is the first species of the genus recorded so far from the Atlantic Ocean, all other described species being western Pacific. A molecular comparison based on a set of concatenated sequences of four markers (three mitochondrial genes (*mtMutS*, *ND2*, and *COI*) and a nuclear segment (*28S*)) relates the species here studied to the published sequences of *Alloptilella splendida*, within the named Clade II of previous general phylogenetic studies on the octocoral Order Pennatulacea. *Alloptilella* is a monophyletic grouping, sister group of the genus *Scytalium* Herklots, 1858. The available molecular information of the genus *Ptilella* Gray, 1870, is reinforced with sequences (*mtMutS*, *ND2* and *28S*) from specimens of *Ptilella inflata* (Kükenthal, 1910) collected off the Namibian coast (SE Atlantic).

Keywords Biodiversity · Coral · Sea pen · Morphology · Molecular analyses · Integrated approach

Introduction

Recent molecular studies in pennatulacean octocorals pointed out the polyphyly of the genus *Pennatula* Linnaeus, 1758 (Dolan et al. 2013; Kushida and Reimer 2018; García-Cárdenas et al. 2020). Two additional contributions proposed nomenclatural acts to resolve that situation: (1) the sequencing of certain North Eastern Atlantic specimens identified as *Pennatula grandis* Ehrenberg, 1834, resulted in the restoration of the old synonymized genus, *Ptilella* Gray, 1870 (García-

Cárdenas et al. 2019); and (2) the existence of a divergent lineage from the genus *Pennatula* (sequences of the type species *Pennatula phosphorea* Linnaeus, 1758, and its close relatives) was corroborated with the description of a new genus based on North Western Pacific material, *Alloptilella* Li, Zhan & Xu, 2021 (Li et al. 2021). In both cases, molecular comparisons helped segregate morphological features previously considered within the morphological variability of the genus *Pennatula* (Kükenthal 1915; Williams 1995).

The morphological description and molecular characterization of *Alloptilella splendida* Li, Zhan & Xu, 2021, force the morphological and molecular revision of controversial material that was preliminary identified as *Pennatula* sp. (GenBank accession numbers DQ302870 for *mtMutS* and DQ302943 for *ND2*) from the Tasman Sea (SW Pacific) deposited at the Northern Territory Museum (Darwin, NT, Australia). This latter material is closely allied (from a molecular point of view) to *Alloptilella*, and was the basis of different discussions concerning the polyphyly of the genus *Pennatula*.

This article is registered in ZooBank under http://zoobank.org/1A5DEA8C-29C1-49DA-AB42-6F2F07AA16FD

Communicated by B. W. Hoeksema

✉ Pablo J. López-González
   pjlopez@us.es

[1] Biodiversidad y Ecología Acuática. Departamento de Zoología, Facultad de Biología, Universidad de Sevilla, Seville, Spain

An additional specimen with a similar morphology and colouration pattern of *A. splendida* was collected during a deep-sea expedition in the North Western Atlantic. This material was deposited at the United States National Museum (Smithsonian Institution, Washington, USA), and the preliminary morphological and molecular study also confirmed its relatedness to the genus *Alloptilella*.

The goal of the present paper is the description of a previously discovered and a new species of the genus *Alloptilella* based on western South Pacific and western North Atlantic specimens, respectively. A morphological and phylogenetic comparison of this material with *A. splendida* was carried out.

Material and methods

The material described here was collected during two different cruises, one of them in the Tasman Sea (RV Tangaroa) and the second one in the Caribbean Sea (NOAA ship Okeanos Explorer). The specimen from the Caribbean Sea was collected by the ROV Deep Discoverer (NOAA).

For comparative purposes, specimens of the morphologically similar genera *Pennatula* and *Ptilella* collected in different survey programmes from the Artic to the Antarctica were also examined: Subantarctic and Antarctic (EASIZ, CLIMANT, BIOROSS), North Eastern Atlantic-Arctic (BIOICE), North Eastern Atlantic (*Scotia* cruises, INDEMARES Chica), South Eastern Atlantic (BENGUELA VIII), and Mediterranean (INDEMARES Cap de Creus, INDEMARES Canal de Menorca, INDEMARES Alborán).

The colonies were fixed on board in ethanol 95% for morphological examination and further molecular studies. Sclerites of different parts of the colonies were prepared for SEM study employing the standard methodology described by different authors (e.g. Bayer and Stefani 1988), and permanent mounts were made for light microscopy. Calyces, tentacles, and other selected fragments were prepared in semi-permanent mounts using clove oil as mounting medium for corroboration of the presence of sclerites and examination of their arrangement in a MOTIC B3 light microscope (Li et al. 2020). Sclerites were mounted on stubs, coated with gold-palladium under a Leica ACE600, and observed with a Zeis EVO SEM at the General Research Services of Microscopy at the University of Seville. Colony and sclerite terminologies mainly follow Bayer et al. (1983) and Li et al. (2021).

Total genomic DNA was extracted from the ethanol (EtOH)-preserved specimen using the E.Z.N.A. DNA kit (OmegaBiotech) following the manufacturer's instructions. Three mitochondrial regions, *mtMutS*, a homologue of the bacterial DNA mismatch repair gene *mutS* (=*msh1*), the NADH-dehydrogenase subunits 2 (*ND2*) and the cytochrome c oxidase subunit I (*COI*), plus a nuclear region, the large subunit ribosomal RNA gene (*28S*) were sequenced. These four markers were concatenated, representing the largest multiloci segment used today in sea pen phylogenies, previous contributions used *mtMutS+ND2* (Dolan et al. 2013; Kushida and Reimer 2018) or *mtMutS+COI+28S* (García-Cárdenas et al. 2020). The start of the *mtMutS* region was amplified using the primers ND42599F and MUT3458R (France and Hoover 2002; Sánchez et al. 2003). The start of the *ND2* region was amplified using the primers 16S47F and ND2-1418R (McFadden et al. 2004). The *COI* region was amplified using the primers COII8068F and COIOCTR (France and Hoover 2002; McFadden et al. 2004). The 28S nuclear ribosomal gene (28S rDNA) was amplified using the primers 28S-Far and 28S-Rar (McFadden and van Ofwegen 2013). Each PCR used 1 U of MyTaq Red DNA Polymerase (Bioline), 10 μM of each primer, approximately 30 ng of genomic DNA, and was brought to a final volume of 25 μL with H_2O for molecular biology (PanReac-AppliChem). *MtMutS* PCR was carried out using the following cycle profile: initial denaturation at 95 °C for 1 min, 35 cycles of denaturation at 95 °C for 15 s, annealing at 55 °C for 15 s, and extension at 72 °C for 10 s, and a final extension at 72 °C for 5 min. The ND2, COI, and 28S PCRs used the same cycle profile, but 51 °C, 58 °C, and 50 °C as annealing temperatures, respectively. PCR products were purified using ExoSAP–IT™ PCR Product Cleanup Reagent (ThermoFisher Scientific) following the manufacturer's instructions, before strong amplifications were sent to Macrogen Spain for sequencing in both directions. All chromatograms were visualized and sequence pairs matched and edited using Sequencher v4.0.

A preliminary Maximum Likelihood (ML) comparison based on *mtMutS* (ca. 400 pennatulacean sequences, not shown) placed the studied taxa here close to a controversial sequence initially attributed to *Pennatula* sp. (GenBank accession number DQ302870, Li et al. 2021, López-González 2021) and the recently proposed genus and species *Alloptilella splendida* (GB MZ198005), within an informally named Clade 2 (Dolan et al. 2013; Kushida and Reimer 2018). These initially identified main Clades were referenced using Roman numerals (as Clade II in this case) by García-Cárdenas et al. (2019, 2020), López-González (2021), and López-González and Drewery (2022). Since that *Pennatula* sp. specimen is studied and identified here as *Pennatula moseleyi* Kölliker, 1880, it is now proposed to be ascribed to the genus *Alloptilella* (see below). This molecular placement is in agreement with morphological features observed in this material, and diagnosed by Li et al. (2021) for the genus *Alloptilella*. Therefore, for the present study, we will only include sequences of Clade II in order to not repeat images and ideas already discussed earlier (Li et al. 2021; López-González 2021). The available molecular information concerning the genus *Alloptilella* covered only *mtMutS* and *ND2* markers (see Dolan et al. 2013 and Kushida and Reimer 2018 as

Pennatula sp.2), but Li et al. (2021) sequenced also *COI* and *28S* when describing *Alloptilella splendida*.

The set of new sequences obtained in this study and those homologous from GenBank (see Table 1) were aligned using MUSCLE, implemented in MEGA 6 (Tamura et al. 2013). The dataset included 43 *mtMutS*, 35 *ND2*, 27 *COI*, and 16 *28S* pennatulacean sequences. According to previous cited molecular phylogenies, the basal resolution of the main sea pen clades is poor. Thus, sequences of two ellisellids from GenBank were selected as an out-group. In addition to the most variable mitochondrial marker (*mtMutS*), three multiloci datasets were analysed: *mtMutS+ND2*, *mtMutS+ND2+COI*, and *mtMutS+ND2+COI+28S*. All the aligned matrices had 45 sequences (43 pennatulaceans and two ellisellids), but varied in the total number of bases: 698 for *mtMutS*, 1239 for *mtMutS+ND2*, 2013 for *mtMutS+ND2+COI*, and 2846 for *mtMutS+ND2+COI+28S*.

The phylogeny reconstruction was obtained by applying Maximum Likelihood and Bayesian inference (BI) methods. After alignment, pairwise genetic distances based on the Kimura 2-parameter (K2P) model of nucleotide substitution (Kimura 1980) were obtained in order to compare them with previous analyses at genus and family levels, following the comparisons of Pante and France (2010), Pante et al. (2012), and López-González (2020). The best nucleotide substitution model was selected using Modeltest implemented in MEGA6, according to Akaike Information Criterion (AIC) and hierarchical likelihood ratio test (hLRT) values. The Maximum Likelihood method was carried out in MEGA6 using the NNI (Nearest Neighbour Interchange) heuristic method and 1000 bootstrap replications. The selected nucleotide substitution model was GTR+G for all multiloci and *mtMutS* matrices. The Bayesian Inference was carried out with MrBayes v3.1.2 (Huelsenbeck and Ronquist 2001; Ronquist and Huelsenbeck 2003), using the substitution model GTR+G (lset nst=6 rates=gamma) and 10^7 generations, and discarding 25% of the initial trees. According to Hillis and Bull (1993), for ML bootstraps, those values <70% should be considered as low, between 70 and 94% moderate, and ≥95% high. According to Alfaro et al. (2003), for Bayesian posterior probabilities, those values <0.95 should be considered as low and ≥0.95 as high. The stationarity of the chains and convergence of the two runs were monitored for each parameter by Tracer (v.1.7.1) (Rambaut et al. 2018), determining whether the effective sample size (ESS) of all parameters was larger than 200, as recommended.

Results

Subclass Octocorallia Haeckel, 1866
    Order Pennatulacea Verrill, 1865
    Family Pennatulidae Ehrenberg, 1834

Genus *Alloptilella* Li, Zhan & Xu, 2021

Diagnosis (slightly modified from Li et al. 2021:1792, modifications in bold)

Colonies **elongated and slender**, pinnate. Axis circular in cross section, present throughout length of colony. Rachis bilaterally symmetrical, with a central dorsal track naked of zooids. Rachis-peduncle limit with a distinct thickening or swelling that forms an edged ring at the thickest point. Polyp leaves large and conspicuous, **narrow to** deltoid, **opposite or** alternately disposed and inserted obliquely, extending ventrally upward. Autozooids in a row along the ventral edge of polyp leaves. Anthocodiae retractile into permanent spiculiferous calyces **alternately placed (giving the false impression of being two series)**. Calyces tubular, **with eight terminal teeth (sometimes of unequal development). Mesozooids in a ridge in continuation of the dorsal base of polyp leaves, and coordinated with siphonozooid patches, basally. Siphonozooids in well-defined patches (V-shaped to check mark-shaped) part on latero-dorsal side of rachis and part between polyp leaves, along the distal insertion of each polyp leaf, on rachis, not on polyp leaves surfaces.** Sclerites as three-flanged needles on calyces, polyp leaves and rachis; inconspicuous three-flanged rods on peduncle and pharynx. **Y-shaped, crossed and 5 or 6 radiates can be present in peduncle, minute bodies ~0.02 mm can also be present.** Three-flanged needles on autozooid tentacles **can be present or absent**.

Distribution and depth

Our knowledge on the distribution of this genus is limited, due to its recent description, the scarce number of collected specimens, the few species currently known and its distant type localities. West Pacific (tropical (~9°N, Y3 seamount), western and central Tasman Sea) and West Atlantic (Puerto Rico, Caribbean Sea); 559 to ~1733 m depth (Kölliker 1880; Li et al. 2021; present account).

Type species

Alloptilella splendida Li, Zhan & Xu, 2021 (by monotypy).

Nominal species

Alloptilella splendida, *Alloptilella moseleyi* comb. nov., and *Alloptilella williamsi* sp. nov.

Remarks

All recent molecular studies failed to recover the monophyly of the family Pennatulidae (e.g. Dolan et al. 2013; Kushida and Reimer 2018; García-Cárdenas et al. 2020;

Table 1 Octocoral species involved in the molecular comparisons carried out in this paper. Specimens and sequences in bold have been obtained for this study

Species name in the tree (specimen code) (or species code: 1, 2)	Catalog Nos. (or additional information)	Geographic area / provenance	$mtMutS$ $(=msh1)$	$ND2$	COI	$28S$
Acanthoptilum gracile (1)	34212-029	NWFSC-west coast	JN866529	-	KF874188	-
Acanthoptilum gracile (2)	34213-027	NWFSC-west coast	JN866544	-	KF874205	-
Actinoptilum molle	RMNH Coel. 40822	n.d.	GQ342491	-	GQ342414	JX203738
***Alloptilella moseleyi*comb. nov.**	**NTM-C014415**	**Tasman Sea-Australia**	DQ302870	DQ302943	**-**	**-**
	BECA (G-3646)		**OL692425**	**OL692430**		
Alloptilella splendida	MBM286413	Tropical W Pacific	MZ198005	-	MZ198007	MZ198009
***Alloptilella williams*isp. nov.**	**USNM 1550625**	**Puerto Rico – NW Atlantic**	**OL692426**	**OL692431**	**OL689028**	**OL689085**
	BECA (G-3491)					
Distichoptilum gracile	NMS.Z.2019.25.2	Whittard Canyon	MK919657	MK919657	MK919657	-
Echinoptilum macintoshi (1)	Isolate YK22	NW Pacific	MK133373	MK133568	-	-
Echinoptilum macintoshi (2)	Isolate YK23	NW Pacific	MK133374	MK133569	-	-
Gilibelemnon octodentatum	BECA (OPEN-452) (G-81)	Seymour Island -Antarctica	MK603841	MW863001	MK603855	MK603851
Pennatula aculeata (1)	NMS.Z.2019.25.7	Whittard Canyon	MK919663	MK919663	MK919663	-
Pennatula aculeata (2)	n.d.	Bay of Biscay	MK919664	MK919664	MK919664	-
Pennatula phosphorea (1)	BECA (OPEN-453) (G-88)	Sea of the Hebrides -NE Atlantic	MK603848	MW863002	MK603858	MK882492
Pennatula phosphorea (2)	BECA OPEN-454 (G-199)	Gulf of Cadiz -NE Atlantic	MK603850	MW863003	MK603861	MK882491
Pennatula sp. 1	BECA (OPEN-152) (G-122)	Ross Sea, Antarctica	MK603849	MW863004	MK603859	MK882493
Protoptilum carpenteri	NMS.Z.2019.25.10	Whittard Canyon	MK919667	MK919667	MK919667	-
Protoptilum sp. (sp. 1)	USNM 94465	Pacific Ocean, Hawaii	DQ297431 EU293804	DQ297450	-	-
Protoptilum sp. (sp. 2)	NHM 2010-20	Eastern Pacific - Monterrey	KF313844	KF313818	-	-
Ptilella grandis (1)	BECA (OPEN-143) (G-92)	South Iceland -NE Atlantic	MK603844	MW863005	MK603860	MK603854
Ptilella grandis (2)	NMS.Z.2019.2.6 BECA (G-69)	Hebridean Shelf -NE Atlantic	MK603843	MW863006	MK882496	MK882494
Ptilella grandis (3)	MZB 2018-0759 BECA (G-138)	Rockall Bank -NE Atlantic	MW862998	MW863007	MW858343	MW862995
Ptilella grayi (1)	BECA (OPEN-340) (G-2591)	Rockall Bank -NE Atlantic	MW862999	MW863008	MW858344	MW862996
Ptilella grayi (2)	NMS.Z.2019.2.2 BECA (G-20)	Rockall Bank -NE Atlantic	MK603846	MW863009	MK603856	MK603853
Ptilella grayi (3)	NMS.Z.2019.2.1 BECA (G-140)	Rockall Bank -NE Atlantic	MK603847	MW863010	MK882497	MK882495
***Ptilella inflata*(1)**	**OPEN-456 (G-124)**	**Namibia -SE Atlantic**	**OL692427**	**OL692432**	**-**	**-**
***Ptilella inflata*(2)**	**MZB 2016-0099 BECA (OPEN-651) (G-3691)**	**Namibia -SE Atlantic**	**OL692428**	**OL692433**	**-**	**OL689086**
***Ptilella inflata*(3)**	**MZB 2016-0105 BECA (OPEN-653) (G-3693)**	**Namibia -SE Atlantic**	**OL692429**	**OL692434**	**-**	**-**
Ptilella cf. *inflata* *	NMS.Z.2019.25.8	Whittard Canyon	MK919666	MK919666	MK919666	-
Ptilosarcus gurneyi (1)	34213-020	NWFSC-west coast	JN866540	-	KF874201	-
Ptilosarcus gurneyi (2)	34210-009	NWFSC-west coast	JN866521	-	KF874180	-
Renilla muelleri	n.d.	n.d.	JX023273	JX023273	JX023273	-
Renilla sp.	CSM-2010-UF4000	E Pacific, Gulf of Panama	GQ342526	-	GQ342455	-
Scytalium herklotsi	USNM 1550636	Puerto Rico -NW Atlantic	MW863000	MW863011	MW858345	MW862997
Scytalium martensi (1)	Isolate YK03	NW Pacific	MK133361	MK133556	-	-
Scytalium martensi (2)	Isolate YK24	NW Pacific	MK133375	MK133570	-	-
Scytalium sp.1 (1)	Isolate YK04	NW Pacific	MK133362	MK133557	-	-
Scytalium sp.1 (2)	Isolate YK06	NW Pacific	MK133363	MK133558	-	-
Scytalium sp.2 (1)	Isolate YK02	NW Pacific	MK133360	MK133555	-	-
Scytalium sp.2 (2)	Isolate YK91	NW Pacific	MK133430	MK133625	-	-
Scytalium veneris	MBM286417	Tropical W Pacific	MZ198006	-	MZ198008	MZ198010
Stachyptilum dofleini (1)	Isolate YK51	NW Pacific	MK133396	MK133591	-	-
Stachyptilum dofleini (2)	Isolate YK52	NW Pacific	MK133397	MK133592	-	-
Stylatula elongata	n.d.	n.d.	JX023275	JX023275	JX023275	-
OUT-GROUP						
Viminella sp.	RMNH Coel.40032 CSM-2012	n.d.	JX203794	-	JX203852	JX203703
Junceella fragilis	n.d.	Taiwan	KJ541509	KJ541509	KJ541509	AF263355

Note that all GenBank sequences are considered here with the names as they appear in GenBank and their original publications (including numbers or letters). Annotations between parentheses (1, 2, … sp.1, sp.2) after the species name are included by the present author just to identify different specimens of a given species or different species under the same denomination in GenBank. Abbreviations: *BECA*, Biodiversidad y Ecología Acuática (Seville, Spain); *CSM*, Collection of Catherine S. McFadden; *MBM*, Marine Biological Museum of Chinese Academy of Sciences (Qingdao, China); *MBM*, Marine Biological Museum of Chinese Academy of Sciences at Qingdao, China; *MZB*, Museu de Zoologia in Barcelona (Spain); *NWFSC*, Northwest Fisheries Science Center (Seattle, USA); *NHM*, Natural History Museum in London; *NMS*, National Museum Scotland Smithsonian (Scotland, UK); *NTM*, Museum and Art Gallery of the Northern Territory (Darwin City, Australia); *RMNH*, Rijksmuseum van Natuurlijke Historie (Leiden, Netherlands); *USNM*, Smithsonian Institution, United States National Museum; *YK*, collection of Y. Kushida; - no data

*This specimen is probably conspecific with *Pt. grandis* (see "Discussion", Fig. 12, and SMFigs.1 and 2).

Fig. 1 *Alloptilella moseleyi* comb. nov. (NTM-C014415); **a** Whole colony, specimen fragmented in four parts; **b** detail of lowermost part of rachis, latero-dorsal, showing dorsal naked track (*ndt*) densely filled with red sclerites, polyp leaves (*pl*) progressively decreasing in size, mesozooids (*msz*) in distinct ridges formed by two lines proximally, but only one distally; **c** detail of a single polyp leaf showing the relatively narrow lateral sides (*pll*), and alternate orientation of autozooids; **d** lateral view of polyp leaves insertion showing lateral view of polyp leaf (*pll*), mesozooid ridge (*msr*), siphonozooid fields (*sph*), under-developed autozooid calyces at the ventralmost polyp leaf edge (*udau*)
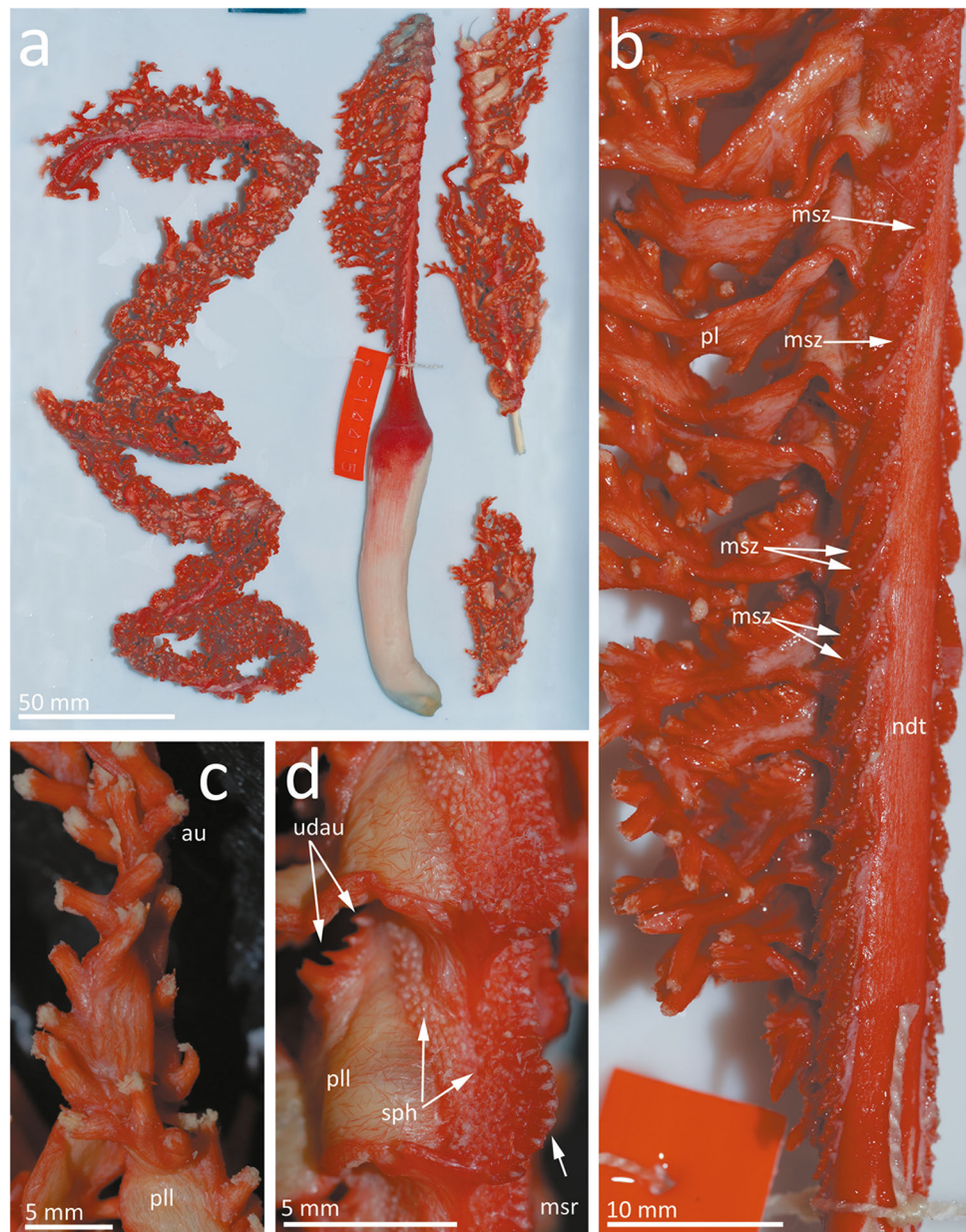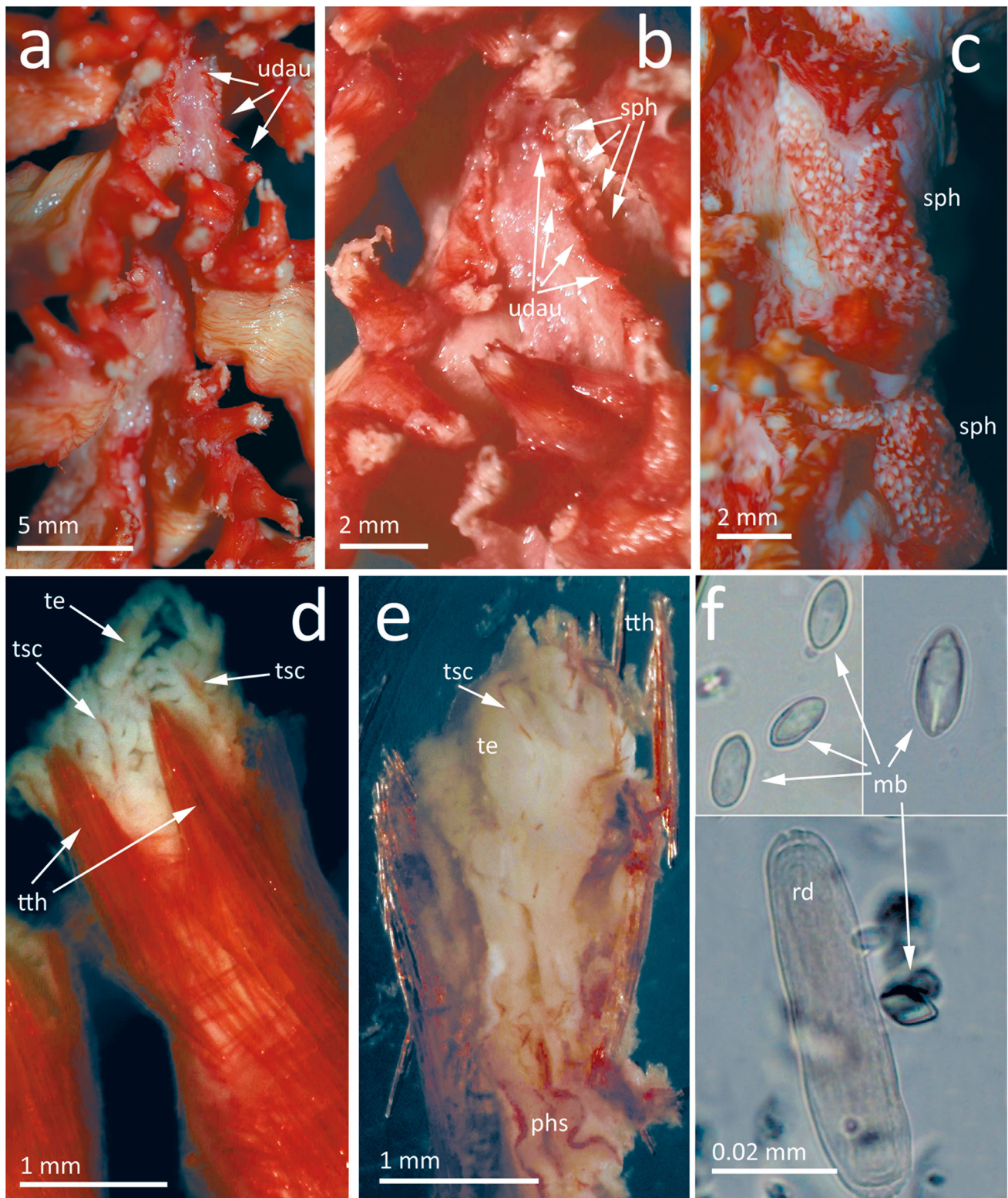
Fig. 2 *Alloptilella moseleyi* comb. nov. (NTM-C014415); **a** and **b** Detail of ventral track showing polyp leaves insertion upwardly directed, underdeveloped autozooid calyces (*udau*) and single line of siphonozooids between two consecutive polyp leaves; **c** rachis, lateral view, showing the "check mark" shape of siphonozooids fields (*msz*), on the right to the dorsal naked track, and on the left those rows placed between consecutive polyp leaves; **d** detail of an autozooid calyx with teeth (*tth*) and autozooid tentacles (*te*) with a narrow band of red sclerites (*tsc*); **e** terminal part of an autozooid cut longitudinally to observe the white tentacles (*te*) with tentacular sclerites (*tsc*), calycular teeth (*dp*), and pharynx with red sclerites (*phs*); **f** detail of sclerites from peduncle (light microscopy) showing minute bodies (*mb*) and rods (*rd*) (see also Figure 5)

López-González 2021; Li et al. 2021). The placement of the genus *Alloptilella* in the family Pennatulidae is here considered for practical reasons, to be in agreement with previous literature, and gross morphologies attributed to *Pennatula*-like forms, there being a need for a more global revision of the family delimitations of the pennatulacean genera reunited in the informally named Clade II.

Alloptilella moseleyi comb. nov. (Kölliker, 1880)
http://zoobank.org/9D34019B-56A6-4A5F-9130-CBFC43A29772

Pennatula moseleyi Kölliker 1880:6-7, Plt. 2 Figs. 8, 9. Kükenthal 1915: 83 (*in text*). Hickson 1916: 183 (*in text*). García-Cárdenas et al. 2019: 266 (*in text*).

Examined material

NTM C014415, Lord Howe Plateau, Tasman Sea, 34° 12.18′S 162° 41.18′E, R.V Tangaroa, 748–772 m depth, 26 May 2003.

Morphological description

Colony pinnate, elongated and erect, approximately 952 mm in length in preserved state, fragmented in four parts (Fig. 1a). Rachis bilaterally symmetrical, 854 mm in length (89.7% of overall length) and 9 mm in width (measured at mid-length of rachis, without polyp leaves), with a moderate thickening at rachis-peduncle limit (10 mm in width), more or less distinct in preserved state (Fig. 1a). Peduncle 98 mm in length (10.3%

Fig. 3 *Alloptilella moseleyi* comb. nov. (NTM-C014415). SEM photographs of sclerites; **a** Calyx, basal parts; **b** calyx, upper part and teeth; **c** tentacle; **d** pharynx; **e** polyp leaves; **f** tentacular sclerites, magnified; **g** pharyngeal sclerites, magnified
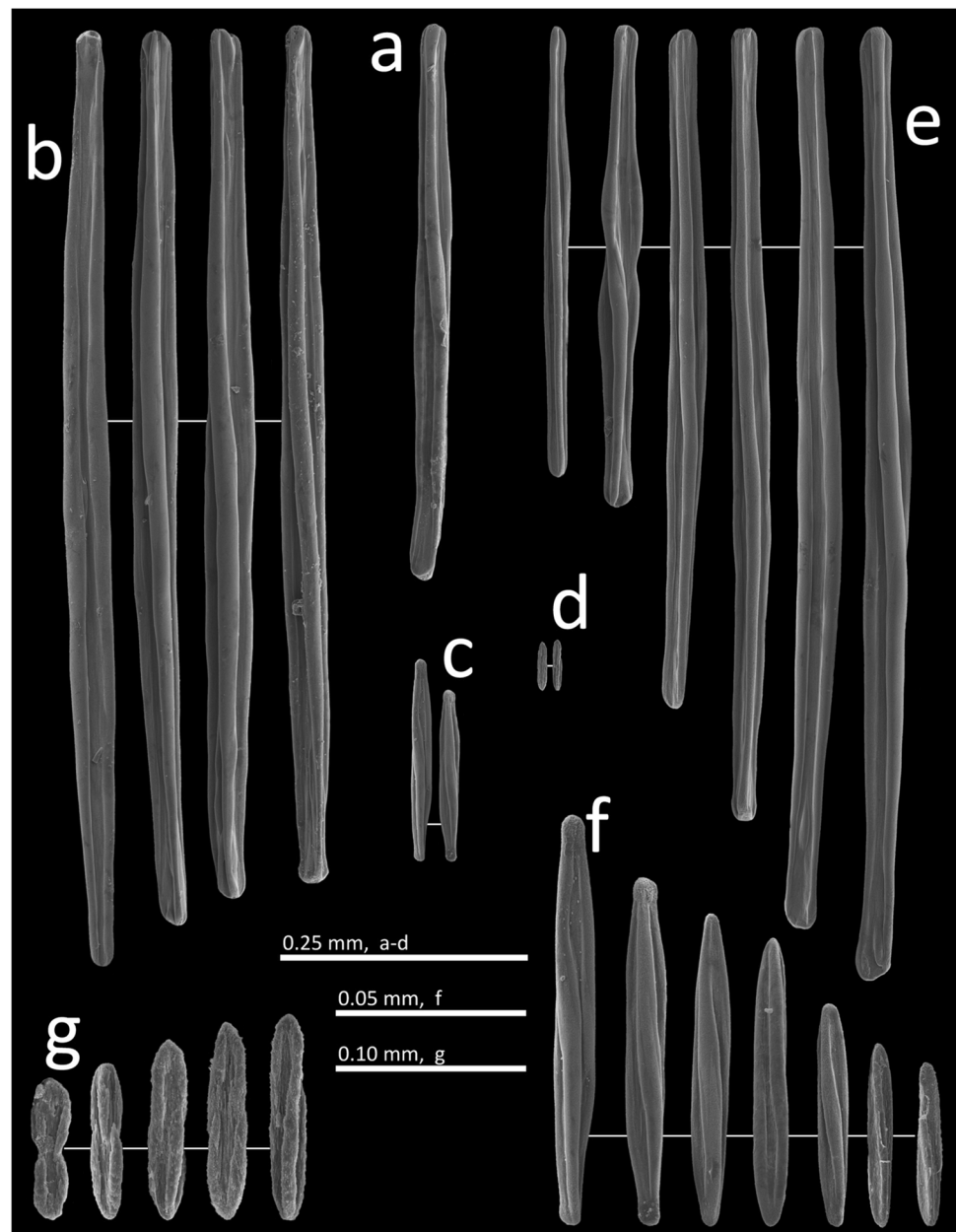
0.25 mm, a-d

0.05 mm, f

0.10 mm, g

of total length). Rachis with a distinctive naked central dorsal track and a hidden ventral track occupied by insertions of polyp leaves. Rachis with approximately 126 pairs of nearly opposite polyp leaves (the fragmented and contracted states of the type make a more accurate count difficult), with the lowest pairs gradually decreasing in size (Fig. 1b), averaging 18 pairs per 100 mm of length (at mid-rachis length). Polyp leaves inserted obliquely, extending ventrally upward. Fully developed polyp leaves narrow in lateral view, maximum length 40 mm, and dorsal edge slightly shorter than ventral edge, maximum width 6 mm (Fig. 1b, c). Axis present throughout colony, circular in cross section, 2.7 mm in diameter measured 12 cm above rachis-peduncle limit (I preferred not to further fragment this specimen looking for the value at the rachis-peduncle limit zone).

Autozooids with calyces, up to 28 in number in the largest polyp leaves, arranged in one row along the ventral edge of each developed polyp leaf (indicated by arrangement of gastrovascular cavities in transversal sections of the polyp leaves), but oriented alternately, appearing falsely to be placed in two rows (Fig. 1c). Anthocodiae retractile into permanent spiculiferous calyces. Calyces tubular, spiculate, armed with 8 strongly projecting teeth, up to 4 mm in length (including teeth) and 1.5 mm in maximum width at basis of teeth level (Figs. 1c and 2d, e), teeth up to 1.6 mm in length (usually around 1.1 mm). Four to six under-developed autozooids on the proximal ventralmost edge of each polyp leaf (Figs. 1d and

Fig. 4 *Alloptilella moseleyi* comb. nov. (NTM-C014415). SEM photographs of sclerites; **a** Polyp leaves; **b** mesozooids; **c** siphonozooids; **d** rachis, dorsal track at mid length; **e** rachis, just above the rachis-peduncle limit
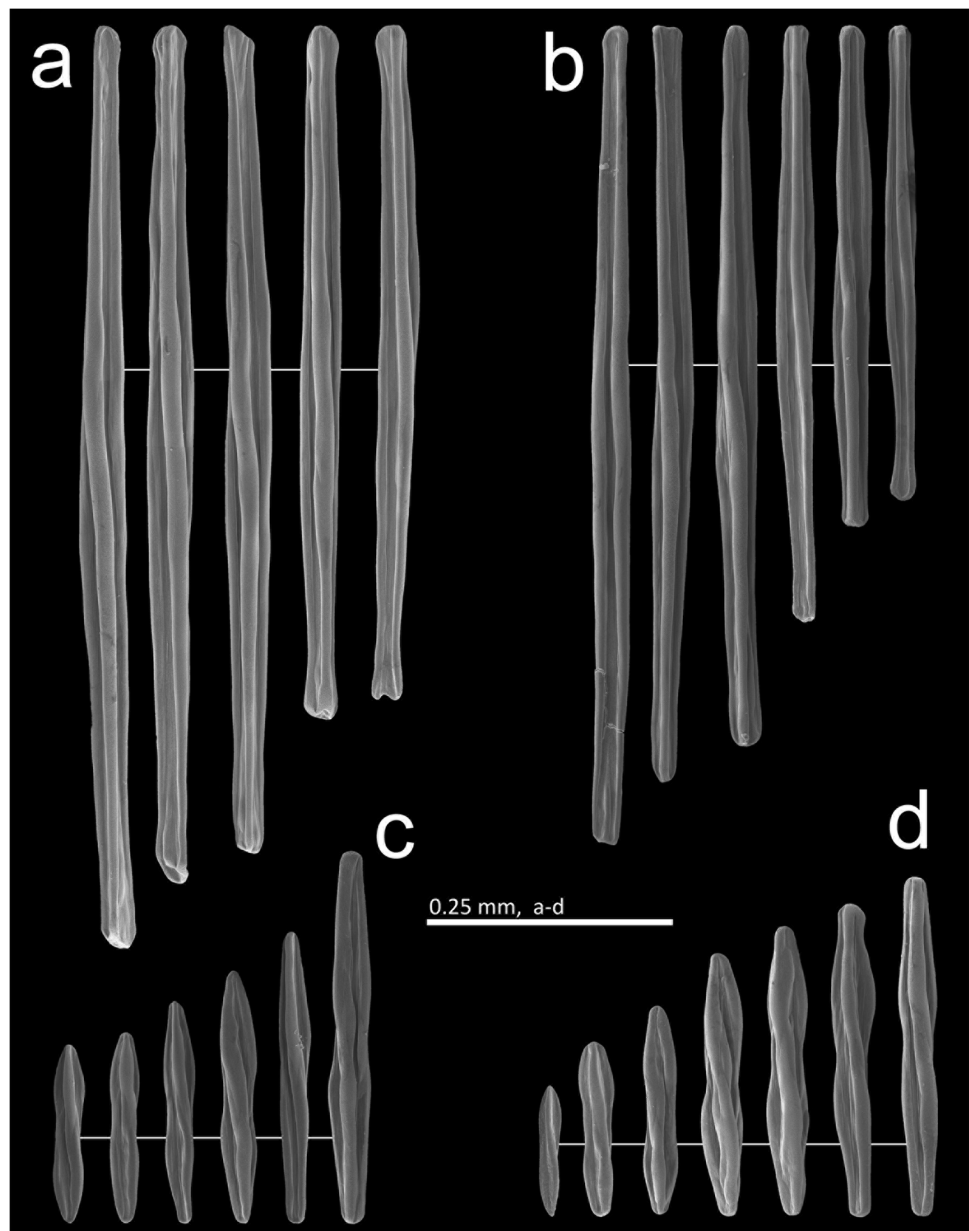
2a, b). Mesozooids distributed on the lateral side of rachis, in an elevated ridge of one line (two lines proximally) (Fig. 1b, c), along the rachis and proximal dorsal edge of polyp leaves, up to 14 in number, decreasing in size from polyp leaf to dorsal track, the last ones of similar size to siphonozooids, the largest one conical, ~1.4 mm in height and 0.8 mm in width, spiculiferous. Siphonozooids minute, 0.17–0.26 mm in diameter (average 0.22 mm, N=20), numerous, arranged in ~10 rows along the axillae of polyp leaves to the latero-dorsal sides of the rachis between polyp leaves, resembling a "check mark" where the long stroke is placed between consecutive polyp leaves (Figs. 1c, d, and 2c), appearing as a single line on the ventral side (Fig. 2b).

Sclerites distributed in various parts of the colony. Densely placed in peduncle, autozooid calices, around mesozooids and siphonozooids openings, and dorsal naked tracks (Figs. 1b, c, and 2c), but widely spaced in lateral (actually they are distal and proximal) sides of polyp leaves (Fig. 2a). Along the aboral side of tentacular axis the sclerites are disposed in a narrow line of 2–3 sclerites (Fig. 2d). Overall, in the proximal part of the rachis, the spicules are more densely packed than in the distal part, and the mesozooid ridges are better defined (Fig. 1b, d).

Sclerites from calyx body as three-flanged needles, up to 0.59 mm in length (Fig. 3a). Sclerites from calycular teeth as three-flanged needles, up to 0.97 mm in length (Fig. 3b). Sclerites from aboral sides of autozooid tentacle axis as three-flanged needles, up to 0.21 mm in length (Fig. 3c, e). Sclerites from autozooid's pharynx as three-flanged needles, up to 0.06 mm in length (Fig. 3d, f). Sclerites from polyp

Fig. 5 *Alloptilella moseleyi* comb. nov. (NTM-C014415). SEM photographs of sclerites; **a** Peduncle, just below the rachis-peduncle limit; **b** peduncle, mid-length, notice minute bodies (*); **c** peduncle, lower end, notice minute bodies (*); **d** and **e** detail from two sclerites from **c**, a three-flanged rod with a minute body (*) and a 6-radiated twinning; **f** magnified minute bodies present in the lower part of peduncle, note also their three-flanged structure
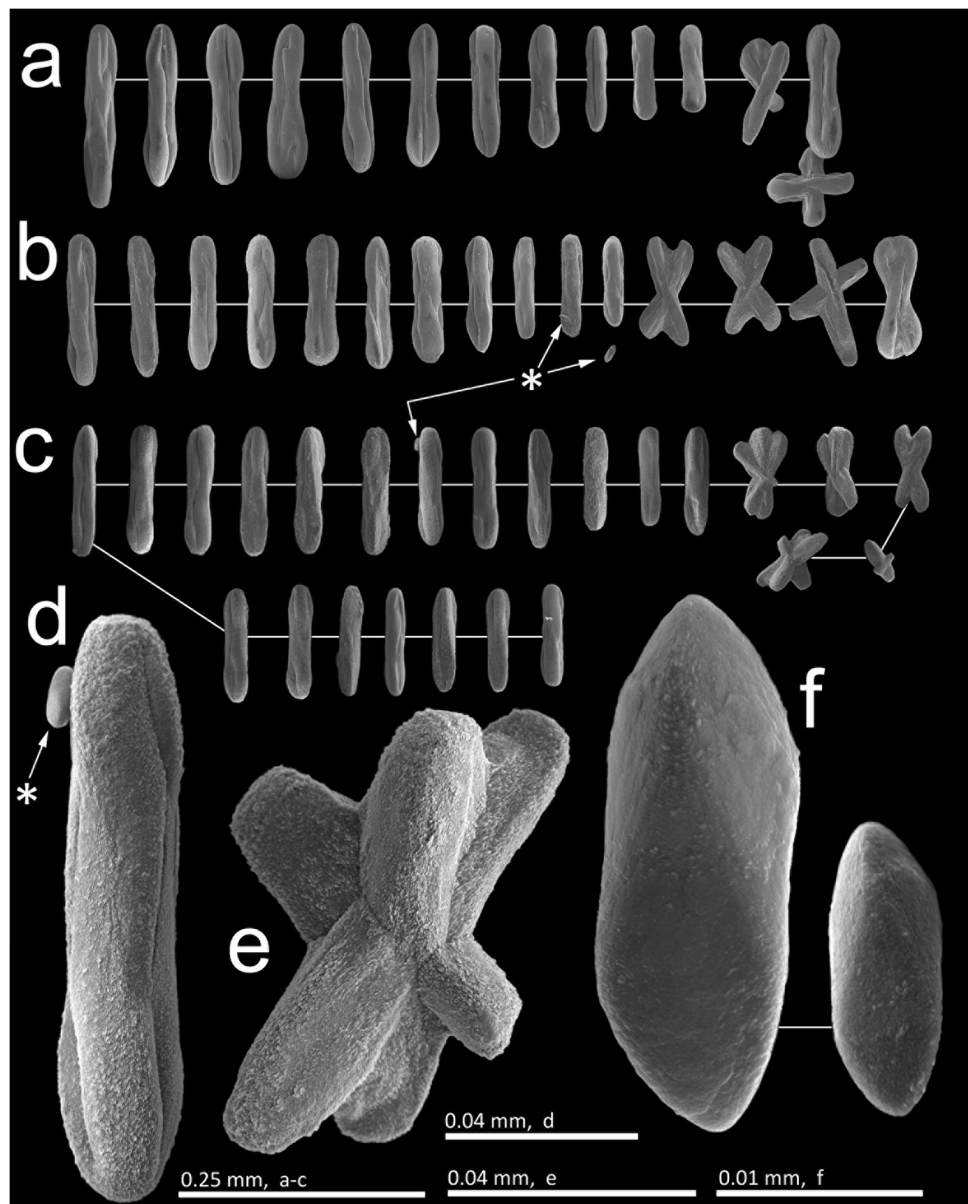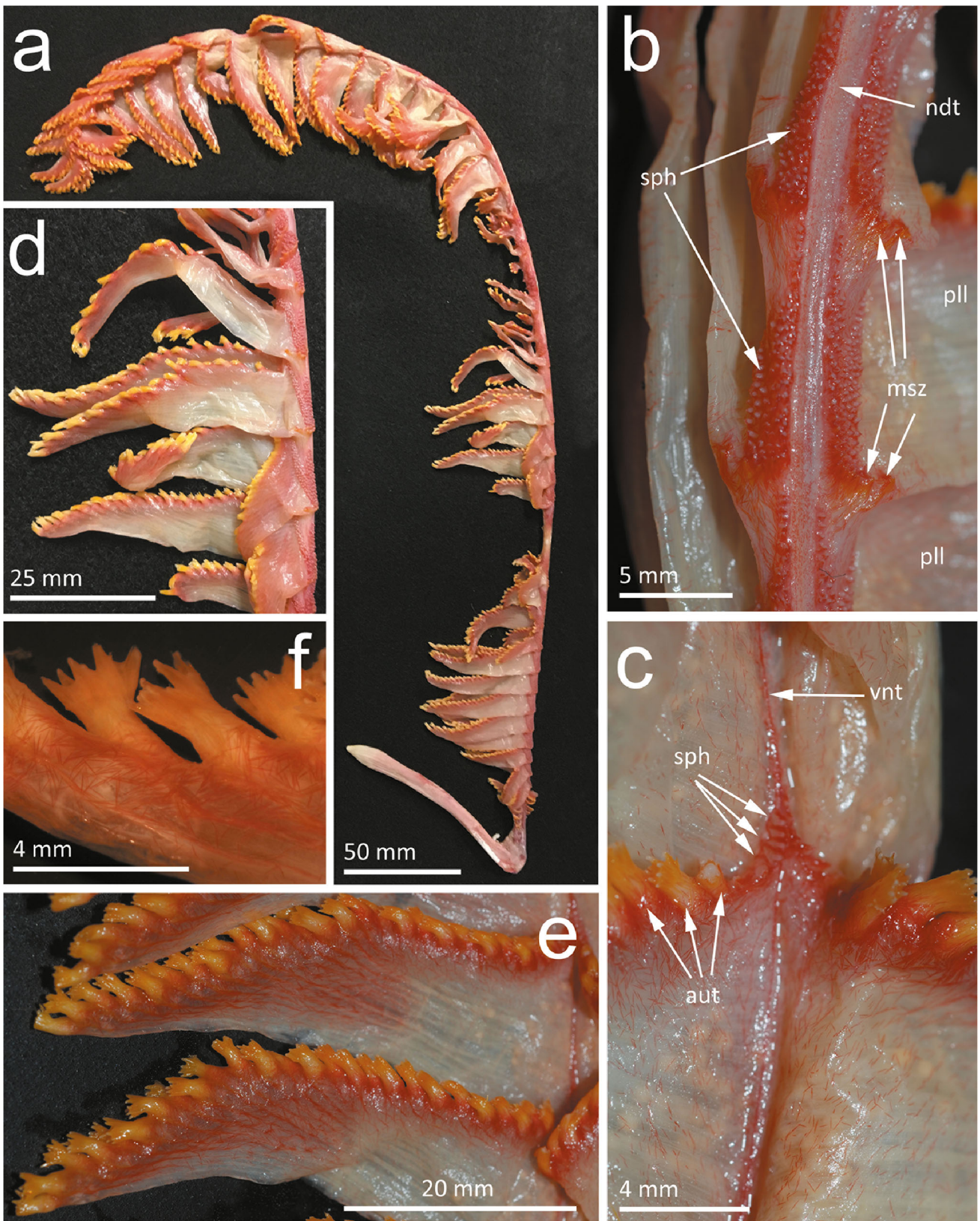
Fig. 6 *Alloptilella williamsi* sp. nov. Holotype (USNM 1550625); **a** Whole colony, specimen damaged at rachis-peduncle limit; **b** detail of naked dorsal track (*ndt*) and latero-dorsal fields of siphonozooids (*sph*), and reduced number of mesozooids (*msz*), one or two of them on the proximal dorsal edge of polyp leaves, and lateral side of polyp leaves (*pll*) showing low density of sclerites, as well as the opposite disposition of polyp leaves; **c** reduced ventral naked track (*vnt*), showing two opposite polyp leaves with reduced in size proximal autozooids (*aut*) and line of single siphonozooids between consecutive polyp leaves (*sph*), note also the low density of red sclerites on the lateral sides of polyp leaves; **d** rachis mid-length in lateral view showing some of the largest polyp leaves; **e** detail of a couple of consecutive polyp leaves (ventral vision of rachis) showing distribution and density of red and yellow sclerites; **f** detail of some autozooid calyces with teeth, notice also the distribution of red sclerites basally. Photos **a** and **d** by T. Coffer USNM

leaves as three-flanged needles, up to 1.1 mm in length (Fig. 3e). Sclerites from mesozooids as three-flanged needles, up to 1.0 mm in length (Fig. 4a). Sclerites from siphonozooids as three-flanged needles, up to 0.9 mm in length (Fig. 4b). Sclerites from mid-rachis dorsal track as three-flanged needles, up to 0.38 mm (Fig. 4c). Sclerites from the lowest part of the rachis, just over the rachis-peduncle limit as three-flanged needles, up to 0.37 mm (Fig. 4d). Sclerites from peduncle as three-flanged rods up to 0.2 mm in length and some crosses up to 0.15 mm in length (Fig. 5a). Sclerites from mid-length of peduncle as three-flanged rods and some crosses, both types up to 0.16 mm in length (Fig. 5b), and a few minute bodies ~ 0.02 mm (see Fig. 5b asterisk). Sclerites from lower basal end of peduncles as three-flanged rods, up to 0.13 mm in length, with numerous crosses, even 3-, 5-, and 6-twinning (Fig. 5c, d, e), and abundant minute bodies ~ 0.02 mm (Figs. 2f, and 5d arrow, f).

Colour

Preserved colony is red, depending on the density of dark red sclerites (Fig. 1a). Red sclerites are present in dorsal track, polyp leaves, autozooid calyces, pharynx, mesozooids, siphonozooids, and aboral side of tentacles. Sclerites from peduncle are reddish at the upper parts and light red to translucent at the mid and proximal ends.

Geographical and depth distribution

At present, *Alloptilella moseleyi comb.* nov. is only known from the southern West Pacific (off Sydney, Australia, 34° 8′ S. 152° 0′ E) and central Tasman Sea (present account), from 748 to ~1737 m depth.

Alloptilella williamsi sp. nov.
http://zoobank.org/8A14ED0C-0EEA-4EFF-A9C8-566DF9BD2EAE

Examined material

USNM 1550625, Holotype, North Atlantic Ocean, Caribbean Sea, Puerto Rico, East of Vieques, EX1811-Dive 02, 18°09′ 59″N 64°59′36″W, 559.10 m depth, 1 Nov 2018. Coll. D. Wagner.

Morphological description of the holotype

Colony pinnate, elongated and erect (Fig. 6a) 620 mm in length in the preserved state (Fig. 6b, c). Rachis bilaterally symmetrical, 53 mm in length (~85% of overall length) and 5 mm in width (measured at mid-length of rachis, without polyp leaves), with a moderate thickening at the rachis-peduncle limit (8 mm in width), more or less distinct in the preserved state (Fig. 6a). Peduncle 90 mm in length (~15% of total length). Rachis with a distinctive naked central dorsal track and a hidden ventral track occupied by insertions of polyp leaves, with a few siphonozooids in the space between consecutive polyp leaves (Fig. 6c). Rachis with approximately 50 pairs of opposite polyp leaves, with the lowest pairs gradually decreasing in size (Figs. 6a, and 7a, c), averaging 8 pairs per 100 mm of length (at mid-rachis length). Polyp leaves inserted obliquely, extending ventrally upward (Fig. 6c, d). Fully developed polyp leaves close to right/obtuse triangular in lateral view, maximum length 50 mm, and dorsal edge slightly shorter than ventral edge, maximum width 20 mm (Fig. 6d, e). Axis present throughout colony, circular in cross section, 4 mm in diameter measured 10 mm above the rachis-peduncle limit.

Autozooids with spiculiferous calyces, up to 29 in number in the largest polyp leaves, arranged in one row along the ventral edge of each developed polyp leaf (indicated by arrangement of gastrovascular cavities in transversal sections of the polyp leaves), but oriented alternately, appearing falsely to be placed in two rows (Figs. 6e, f, and 7c, d, e, f). Anthocodiae retractile into permanent spiculiferous calyces. Calyces tubular but wider distally, spiculate, armed with 8 strongly projecting teeth (sometimes of different development), up to 4.1 mm in length (including teeth) and 1.7 mm in maximum width at basis of teeth level (Figs. 6f, and 7d, e, f), teeth up to 0.95 mm in length (usually around 0.8 mm). Autozooids of lowermost polyp leaves increasing in size from proximal to distal in the polyp leaf, quickly reaching a high number of calyces (Fig. 7b). Mesozooids distributed on the dorsal side of the rachis, in a low ridge of a single line (rarely two in the proximities of the polyp leaf base), along the rachis and proximal dorsal edge of polyp leaves, ~14 in number (coordinated with the lowermost polyp leaves, see Fig. 11e), decreasing in number from the proximal to the distal part of the rachis, decreasing in size from
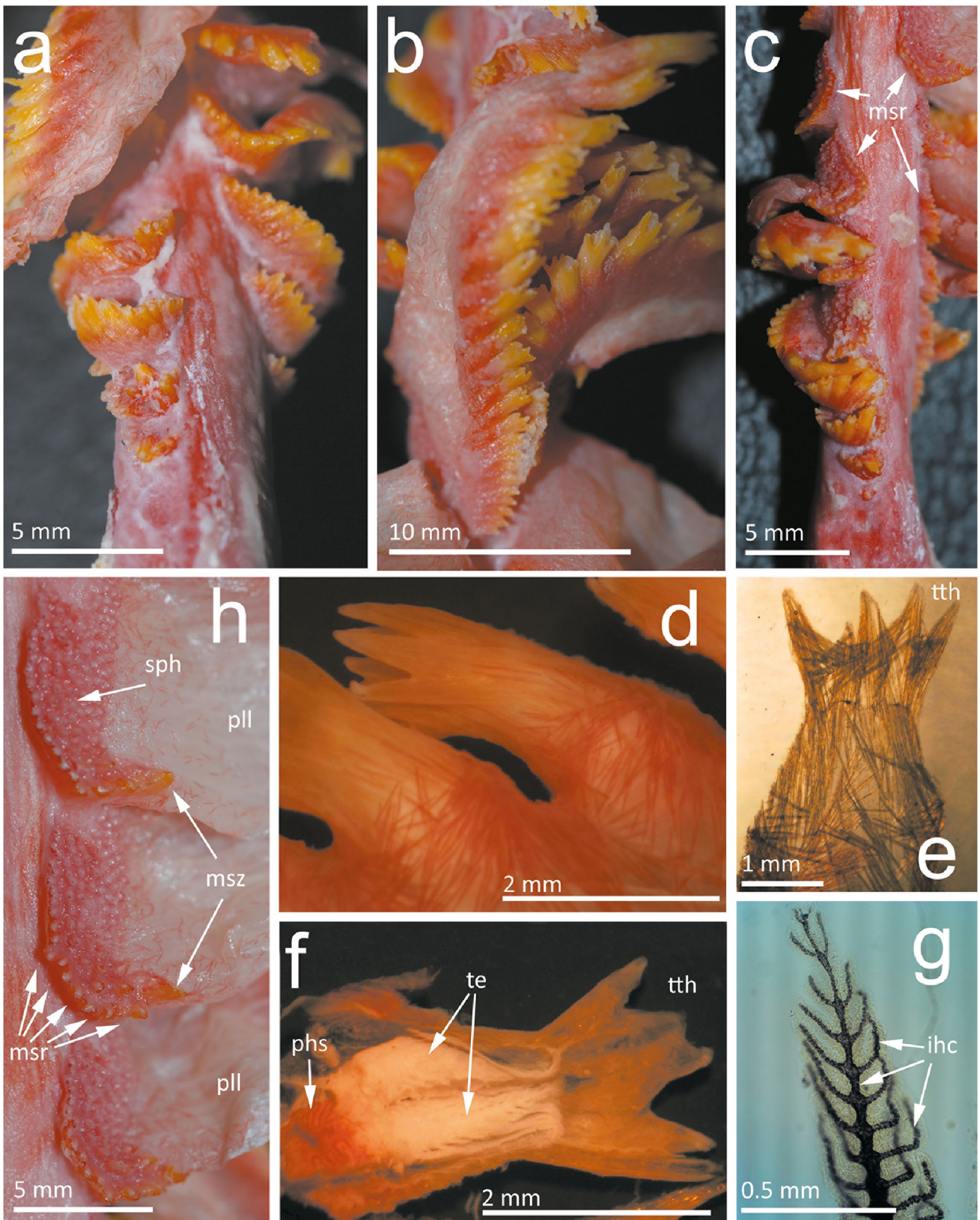
Fig. 7 *Alloptilella williamsi* sp. nov. Holotype (USNM 1550625); **a** Detail of the rachis-peduncle limit, latero-ventral view, showing the progressive decreasing size of polyp leaves; **b** detail of one of the nearly full-developed polyp leaves at the proximal part of rachis, showing the progressive reduction in size of autozooid calyces; **c** detail of the rachis-peduncle limit, latero-dorsal view, showing the progressive decreasing size of polyp leaves, the larger size of autozooid at dorsal placements, and the pronounced mesozooid ridges (*msr*); **d** detail of autozooid calyces, notice teeth and red sclerites basally; **e** part of an autozooid calyx cut longitudinally in clove oil to observe sclerite arrangement and unequal development of calycular teeth (*tth*); **f** distal part of autozooid cut longitudinally, showing unequal development of teeth (*tth*), tentacles without sclerites (*te*), and pharynx with red sclerites (*phs*); **g** half-distal part of a tentacle in clove oil showing internal hollow canals (*ihc*) along main tentacular axis and pinnulae, as well as absence of sclerites; **h** dorsal view of mesozooid ridges (*msr*) coordinated with siphonozooid (*sph*) fields of three consecutive polyp leaves, notice yellow colour of large mesozooids (*msz*) on the dorsal proximal edge of polyp leaves, and the scarce density of red sclerites on its lateral sides (*pll*)

polyp leaf to dorsal track, the last ones of similar size to siphonozooids, difficult to distinguish (Fig. 7h). One of the two largest ones is conical, on the proximal part of the dorsal edge of polyp leaves, approximately up to 1.5 mm in height and 0.5 mm in width, spiculiferous (Figs. 6b, 7h, and 11d arrows). Siphonozooids minute, 0.2–0.3 mm in diameter (average 0.24 mm, $N=20$), numerous, arranged in approximately up to 6–8 rows dorsally, along the axillae of polyp leaves to the latero-dorsal sides of the rachis between polyp leaves, resembling a "check mark" where one of the strokes is placed between consecutive polyp leaves, and the other runs dorsally, proximally limited by the ridge of mesozooids (Figs. 6b, 7h, and 11d, e, f). Siphonozooids usually do not form a continuous band dorsally, each dorsal "patch" decreases in the number of rows until just a single one, the band running between consecutive polyp leaves also decreases in number of rows, ending in a single one, which reaches the ventral track (Fig. 6c).

Sclerites distributed in various parts of the colony. Sclerites are densely placed on peduncle, around mesozooid and siphonozooid openings (Fig. 6b), but widely spaced in dorsal naked tracks (Fig. 6b), lateral (actually they are distal and proximal) sides of polyp leaves (Fig. 6c). Sclerites are completely absent along the aboral side of tentacular axis and pinnulae (Fig. 7f, g).

Sclerites from calyces body as three-flanged needles, up to 0.6 mm in length (Fig. 8a). Sclerites from calycular teeth as three-flanged needles, up to 1.2 mm in length (Fig. 8b). Sclerites from autozooid's pharynx as three-flanged needles, up to 0.06 mm in length (Fig. 8c, d). Sclerites from polyp leaves as three-flanged needles, up to 0.75 mm in length (Fig. 9a). Sclerites from mesozooids as three-flanged needles, up to 0.95 mm in length (Fig. 9b). Sclerites from siphonozooids as three-flanged needles, up to 0.57 mm in length (Fig. 9c). Sclerites from the mid-rachis dorsal track as

three-flanged needles, up to 0.13 mm (Fig. 9d). Sclerites from the lowest part of rachis, just above the rachis-peduncle limit as three-flanged needles, up to 0.14 mm (Fig. 9e). Sclerites from peduncle as three-flanged rods (sometimes pointed, flanges mainly noticeable at the ends, often simply as slits) and some Y-shaped and crosses, up to 0.055 mm in length (Fig. 10a, b). Sclerites from mid-length of the peduncle are similar in shape diversity and size to that of the upper part, 5 or 6 radiated can be present (Fig. 10c, d). Sclerites from the lower distal end of the peduncle mainly as minute bodies (~0.02 mm) and scarce rods of similar shape and size to those in the upper parts of the peduncle.

Colour

The preserved colony is reddish, depending on the density of dark red sclerites (Figs. 6a and 11). Red sclerites are present in dorsal track, polyp leaves, basal part of autozooid's calyces, pharynx, and siphonozooids. Sclerites from distal part of calyces, including calycular teeth, are yellow. Sclerites from mesozooids are mainly yellow, but some reddish and some bicoloured (ends yellow and centre red) are also present. Sclerites from the peduncle are light red to translucent in colour.

Living habitus and environment

The holotype of *Alloptilella williamsi* sp. nov. was collected by the ROV *Deep Discoverer* (Fig. 11a) (see also all photographic information associated with the registration code USNM 1550625 on the Web site "Search the Department of Invertebrate Zoology Collections" of the of the Smithsonian Institution, National Museum of Natural History (https://collections.nmnh.si.edu/search/iz/)). The fully expanded specimen (Fig. 11b) combining the deep and light red colours (depending on the density of red sclerites) with the distinct series of yellow autozooids on the ventral edge of polyp leaves, as well as the yellow ridges of mesozooids on latero-dorsal surfaces (Fig. 11d–e), the rachis peduncle limits (Fig. 11e) is moderately expanded, as well as the polyp-free dorsal track and mid to lower polyp leaves (Fig. 6e). The autozooids, placed in a single row on the ventral edge of polyp leaf, are alternatively oriented (see Fig. 6c). The rachis of the type material presents damages at mid-length, probably due to extractive human activities on these bottoms, showing also clear signs of recovery (Fig. 11c). According to the expedition report (Wagner et al. 2019: p. 72), the habitat observed during the EX1811-Dive02 included moderate slopes with thin sediment (Fig. 11b), associated benthic fauna included, apart from some sponges (hexactinelids and demosponges) and the abundant echinoderms (crinoids, cidarids, brittle stars, and sea stars), hydrocorals, octocorals, antipatharians, and solitary scleractinians (not in high density). The octocorals

Fig. 8 *Alloptilella williamsi* sp. nov. Holotype (USNM 1550625). SEM photographs of sclerites; **a** Calyx, basal parts; **b** calyx, upper part and teeth; **c** pharynx; **d** pharyngeal sclerites, magnified
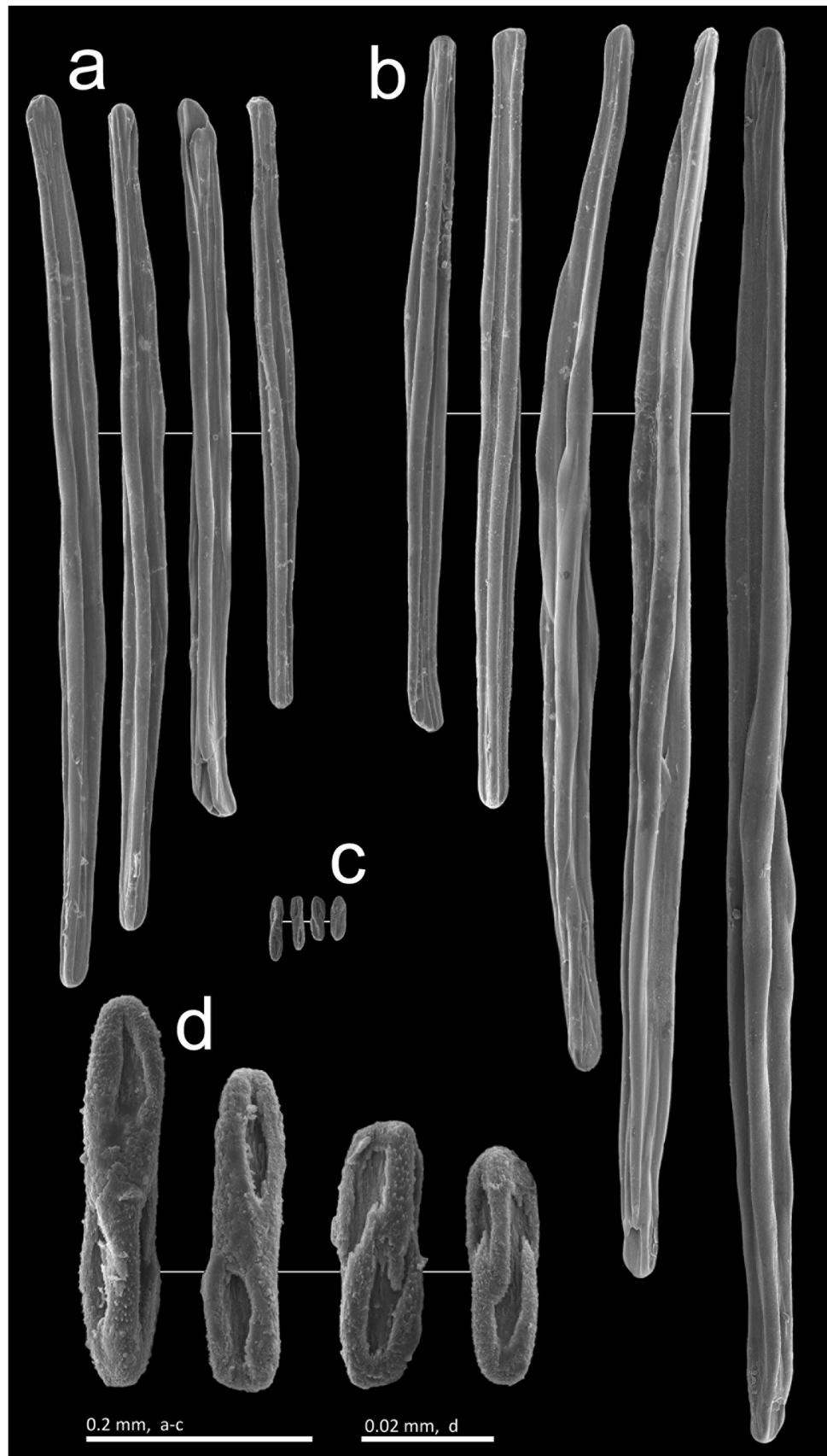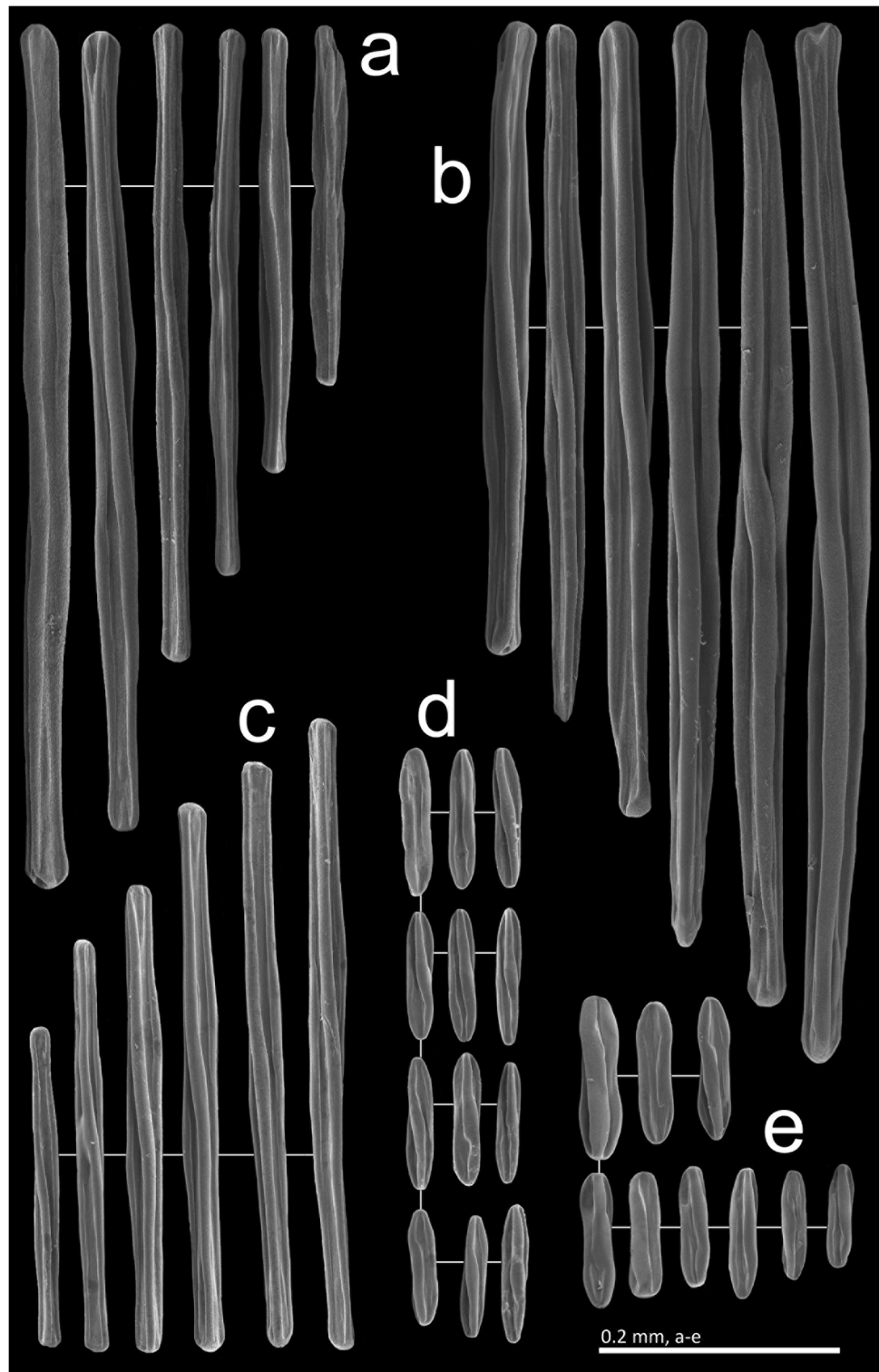
Fig. 9 *Alloptilella williamsi* sp. nov. Holotype (USNM 1550625). SEM photographs of sclerites; **a** Polyp leaves; **b** mesozooids; **c** siphonozooids; **d** rachis, dorsal track at mid-length; **e** rachis, just above the rachis-peduncle limit


observed in this dive included plexaurids (*Thesea* sp.), primnoids (*Acanthoprimnoa* sp., *Callogorgia* sp.), isidids s.l. (bamboo corals) (see Saucier et al. 2021 for the current placement of the different genera previously considered in the family Isididae Lamouroux, 1812), and chrysogorgiids.

Etymology

The species epithet is chosen in honour of Dr. Gary C. Williams, curator of invertebrates at the California Academy of Sciences (California, USA), in recognition of his important

Fig. 10 *Alloptilella williamsi* sp. nov. Holotype (USNM 1550625). SEM photographs of sclerites; **a** Peduncle, just below the rachis-peduncle limit; **b** cross from **a**, magnified; **c** peduncle, mid-length; **d** rods and cross from **c**, magnified
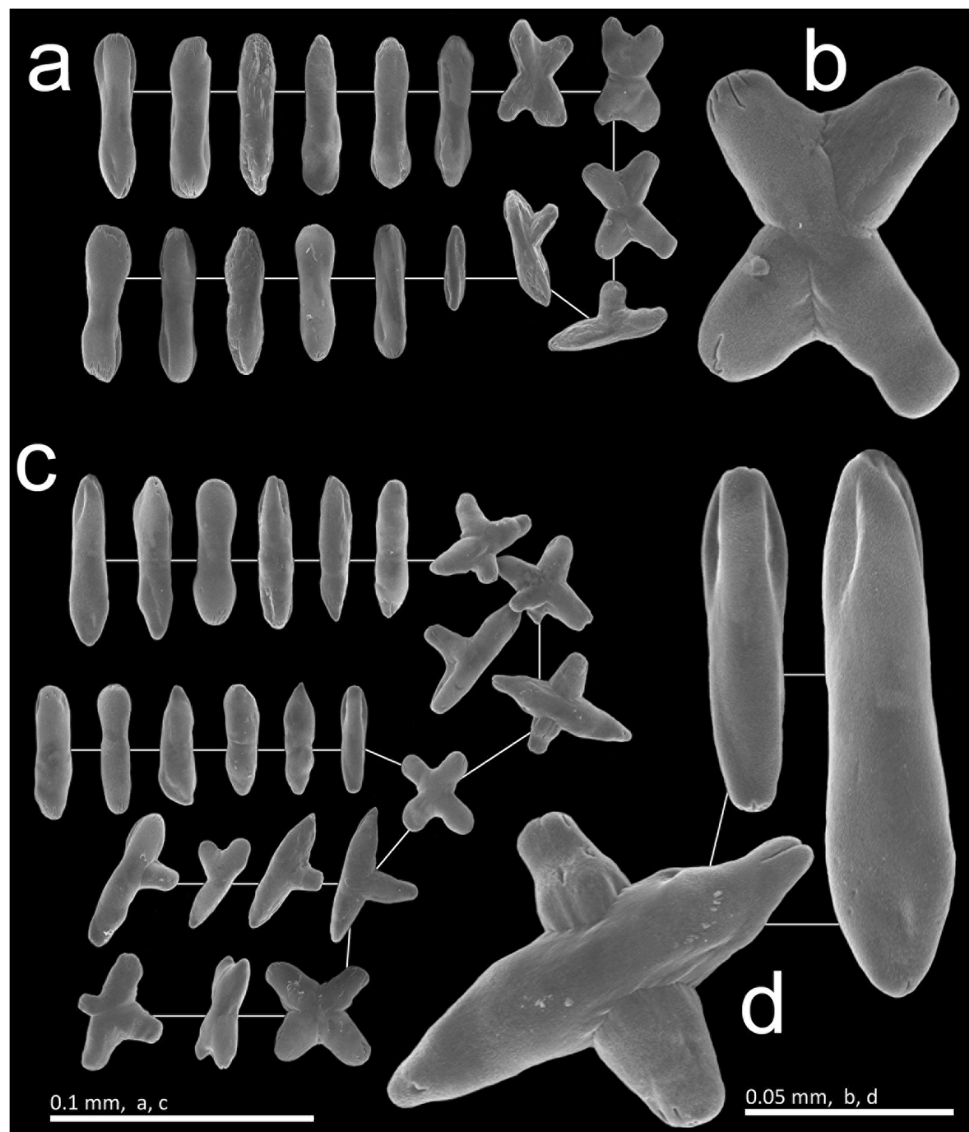
contribution to our knowledge of pennatulacean diversity and worldwide distribution (Williams 2011).

Geographical and depth distribution

At present, *Alloptilella williamsi* sp. nov. is only known from the Caribbean Sea (NW Atlantic) from 559.10 m depth.

Bootstrap (Bst) and Posterior Probability (PP) values (Bst) and Posterior Probability (PP) values

Phylogenetic analyses

In the *mtMutS+ND2+COI+28S* hypothesis (Fig. 12), the BI and ML topologies are identical. The multiloci sequences obtained for *Allopitlella moseleyi* comb. nov and *A. williamsi* sp. nov. were reunited in a distinct and well-supported clade (Bootstrap (Bst) 99%, Posterior Probability (PP) 1) with other multiloci sequences

recently published as *Alloptilella splendida*, the type material of the type species of the genus *Alloptilella*. *Alloptilella* is then easily identifiable as a monophyletic genus, being the sister group of all sequences of another distinctly morphological and molecular genus, *Scytalium* Herklots, 1858. *Alloptilella* and *Scytalium* are in a well-supported clade (Bst 97%, PP 1) which is the sister group of a poorly supported *Ptilella-Distichoptilum* clade (Bst 29%, PP 0.51). The position of the genus *Pennatula* in this phylogenetic hypothesis is distinctly separated from *Ptilella* and *Alloptilella*, *Ptilosarcus* being the sister group of *Pennatula*, with a low to moderate support from the ML inference (Bst 68%), but a high support (PP 0.99) from the Bayesian inference. Different genera currently included in the families Renillidae (*Renilla*), Virgulariidae (*Acanthoptilum, Actinoptilum*), and Stachyptilidae (*Gilibelemnon*) are placed in between the *Pennatula-Ptilosarcus* and the *Ptilella-Distichoptilum* and *Alloptilella-Scytalium* subclades (see Fig. 12).

The topologies obtained using the BI and ML methods for the *mtMutS*, *mtMutS+ND2*, and *mtMutS+ND2+COI* hypotheses are almost identical (SMFigs. 1, 2), and somewhat more resolved (but moderately supported) in the multiloci datasets. The three genera discussed here (*Pennatula*, *Ptilella*, and *Alloptilella*) are well supported in all BI trees (PP 1), while Bst values (ML trees) varied depending on the dataset used (98, 91, and 94% for *Pennatula*; 100, 99, and 100% for *Ptilella*; and 92, 99, and 96% for *Alloptilella*, for each of the above listed hypotheses, respectively).

In the *mtMutS* tree (SMFig. 1, left), species distinction is not always observed for all *Ptilella* and *Alloptilella* species. The three *Pennatula* species used for this tree are clearly differentiated, while *P. grandis* and *P. inflata* share identical sequences, and only *P. grayi* is differentiated. Concerning *Alloptilella* species, *A. moseleyi* comb. nov. and *A. williamsi* sp. nov. share the same sequence, and then, only *A. splendida* is differentiated. As in the four markers hypothesis, *Scytalium* is the sister group of *Alloptilella* (PP 1, Bst. 96%).

In the *mtMutS+ND2* hypothesis (SMFig. 1, right), the topologies of the BI and ML trees are also very similar and are in general agreement with the *mtMutS* hypothesis. However, in this case, all the *Ptilella* and *Alloptilella* species are differentiated (more clearly visible in *Ptilella*, where at least three colonies per species are sequenced). *Ptilella grandis* and *P. inflata* are sister groups (PP 1, Bst 96%), and they are the sister group of *P. grayi* (PP 1, Bst 99%). A specimen identified as *P.* cf. *inflata* from eastern North Atlantic (GenBank MK919666, complete mitochondrial sequence) is here clearly aligned with *P. grandis*. *Ptilella inflata* is recognized as a southern West Indian species, also present in South Africa and Namibia (Kükenthal 1910; Williams 1995; López-González et al. 2001). The present sequenced colonies of *P. inflata* were collected off Namibian coasts, 418–439 m in depth (López-González et al. 2001). In this hypothesis, *Alloptilella* species are minimally differentiated from a molecular point of view (see "Discussion") forming a polytomy. As in the *mtMutS* hyphothesis, *Pennatula* species are well defined.

A phylogenetic hypothesis considering only mitochondrial markers (*mtMutS+ND2+COI*) have the same main topology, but is reinforced at species level by the additional differences in *COI* marker (SMFig. 2). *Ptilella* and *Pennatula* species remain well separated, while *Alloptilella* species also maintain the same polytomy observed in *mtMutS* and *mtMutS+ND2* hypotheses.

In a selected dataset considering only *mtMutS*, uncorrected *p*-distances indicate that the average genetic distance within *Alloptilella* species is 0.1% (having only the values of 0.0% or 0.2%). *Alloptilella moseleyi* comb. nov. is 0.0% and 0.2% distant from *Alloptilella williamsi* sp. nov. and *A. splendida*, respectively. *Alloptilella williamsi* sp. nov. is 0.2% distant from *A. splendida*. At the immediately higher taxonomic level (genus level) and now using the K2 nucleotide substitution model, *Alloptilella* is 3.3% (range 3.1–3.6%) distant from *Ptilella*, and 4.5% (range 4.3–4.7%) distant from *Pennatula*, while *Pennatula* is 3.6% (range 3.4–3.7%) distant from *Ptilella*. Finally, *Alloptilella* is 4.9% (range 3.7–5.4%) distant from *Scytalium*, its sister group.

In order to provide additional comparison, the most common multiloci dataset previously analysed in pennatulacean phylogenetic papers (*mtMutS+ND2* and *mtMutS+COI+28S*) has also been explored using the K2 nucleotide substitution model (see SMTables 1 and 2). In the *mtMutS+ND2* data matrix, the mean intraspecific genetic distances in *Alloptilella*, *Ptilella*, and *Pennatula* are 0.08%, 0.33%, and 0.27% respectively, while *Alloptilella* is 2.22% distant from *Ptilella* and 3.61% distant from *Pennatula*, and *Pennatula* is 2.96% distant from *Ptilella* (see SMTable 1 for ranges). In the analysis of the *mtMutS+COI+28S* data matrix, the mean intraspecific genetic distances in *Alloptilella*, *Ptilella*, and *Pennatula* are also low at 0.02%, 0.39%, and 1.06%, respectively, while *Alloptilella* is 27.62% distant from *Ptilella* and 29.11% distant from *Pennatula*, and *Pennatula* is 9.54% distant from *Ptilella* (see SMTable 2 for ranges). A final analysis including the multiloci *mtMutS+COI* (SMTable 3) corroborates the idea that genetic distances at genus level are improved by the inclusion of the *28S* segment, as overall genetic distances are similar and of the same order of magnitude as those obtained using the *mtMutS+ND2* dataset.

Artificial key to *Alloptilella* species (see also Table 2 for a complete comparison of morphological characters)

1. Colony red in colour (spicules of distal part of calyces and mesozooids are also red in colour); with sclerites on the tentacular axis ……………………….…………………….……………….……….……….…………. *Alloptilella moseleyi* comb. nov.
- Colony red and yellow in colour (spicules of distal part of calyces and mesozooids are yellow in colour); with or without sclerites on the tentacular axis **2**
2. Polyp leaves in an alternate disposition; with sclerites on the tentacular axis …………………............…... *Alloptilella splendida*
- Polyp leaves in an opposite disposition; without sclerites on the tentacular axis ……………..... *Alloptilella williamsi* sp. nov.
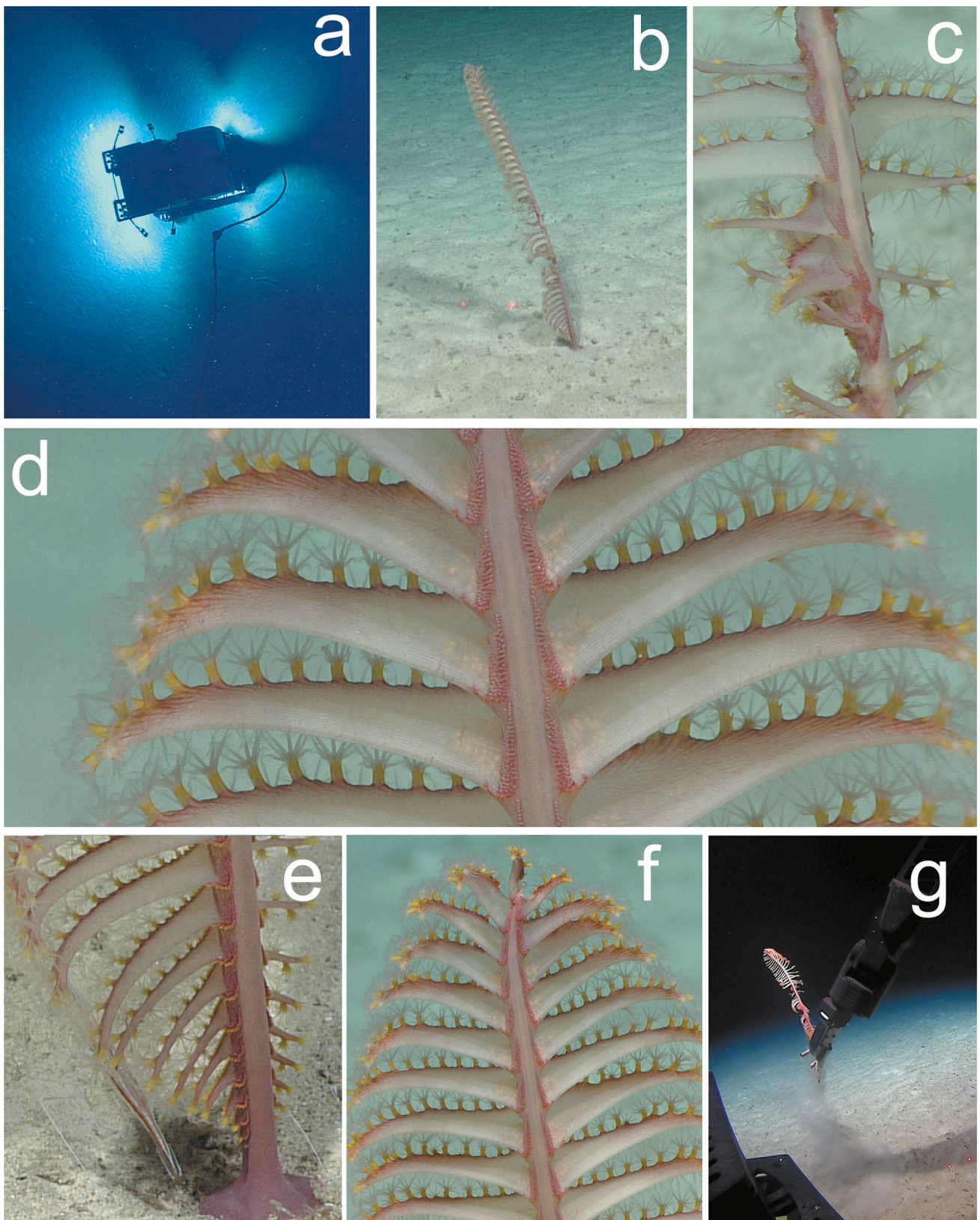
◀ **Fig. 11** In situ photographs of *Alloptilella williamsi* sp. nov. Holotype (USNM 1550625); **a** ROV *Deep Discoverer* on the bottom during the captures of the type material of *A. williamsi* sp. nov.; **b** whole extended colony (lasers are 10 cm apart), notice damage at the mid-rachis length; **c** detail of damage on the rachis; **d** detail of the upper part of rachis, polyp leaves extended, notice the shape of siphonozooid fields, alternate orientation of autozooids, low density of sclerites on the polyp leaves' lateral surfaces, and poor development of mesozooid ridges, notice one or two mesozooids on the proximal dorsal edge of each polyp leaf (arrows); **e** detail of the expanded rachis-peduncle limit and lowest polyp leaves, notice the progressively decreasing size of polyp leaves, and the well-developed and yellow-coloured mesozooid ridges; **f** general view of the distal part of rachis, showing the opposite disposition of polyp leaves; **g** precise moment of collection by the arm of the ROV *Deep Discoverer*. Photos by NOAA Office of Ocean Exploration and Research (see all photos associated with the registration code USNM 1550625 on the Web site "Search the Department of Invertebrate Zoology Collections" of the Smithsonian Institution, National Museum of Natural History (https://collections.nmnh.si.edu/search/iz/))

Discussion

The sequences in GenBank identified as *Pennatula* sp. (DQ302870 for *mtMutS* and DQ302943 for *ND2*) belong to the same material here identified as *Pennatula moseleyi* Kölliker, 1880. According to the current knowledge, the assignation of this material to Kölliker's species is reasonable, and is also the most conservative proposal. This species is transferred here to the genus *Alloptilella* as *A. moseleyi* comb. nov. Due to its controversial position in the published phylogenetic trees (e.g. Dolan et al. 2013; Kushida and Reimer 2018; García-Cárdenas et al. 2020; López-González 2021; Li et al. 2021), total DNA of that specimen was extracted and sequenced again for this paper; only the previously known segments (*mtMutS* and *ND2*) were successfully amplified and

Fig. 12 Bayesian analysis showing the phylogenetic relationships of *Alloptilella moseleyi* comb. nov. and *Alloptilella williamsi* sp. nov. with *Alloptilella splendida* and other related genera and species of sea pens within Clade II. The present hypothesis is based on the concatenated set of sequences of four markers: *mtMutS+ND2+COI+28S*. The tree is drawn to scale, with branch lengths measured in the number of substitutions per site. Supporting values of nodes as Bootstrap (%)/Posterior Probability. See Table 2 for complete list of species and GenBank accession numbers. *This specimen is probably conspecific with *P. grandis* (see "Discussion", SMFigs.1 and 2)
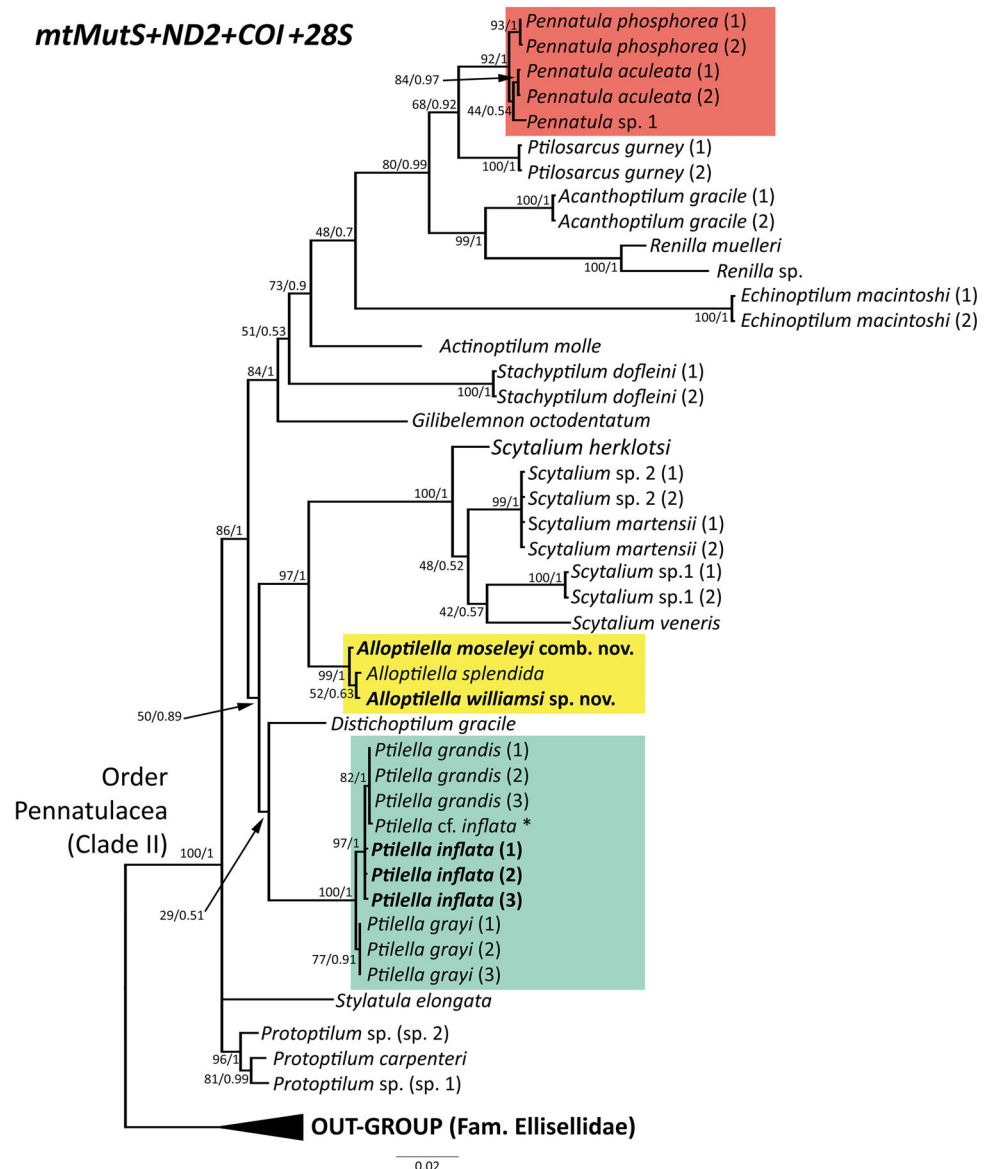
Table 2 Comparative table of *Alloptilella* species discussed in this paper. *Alloptilella* species are listed according to their date of description. Notes: *n.d.*, no data; (1) Kölliker (1880: p. 6); (2) Li et al. (2021: 1792); (3) this paper

Characters / species	A. *moseleyi* comb. nov.[1,3]	A. *splendida*[2]	A. *williamsi* sp. nov.[3]
Ventral track	Naked, narrow, hidden occupied by insertions of polyp leaves	Naked, narrow, hidden occupied by insertions of polyp leaves	With a few siphonozooids from the line running between consecutive polyp leaves, easy to confuse with under-developed autozooids. Ventral track narrow, as a line, hidden occupied by insertions of polyp leaves
Dorsal track	Naked throughout length of rachis	Naked throughout length of rachis	Naked throughout length of rachis
Maximum number of polyp-leaf pairs and distribution (colony size)	126 pairs of nearly opposite polyp leaves, averaging 18 pairs per 100 mm in length (952 mm)	65 pairs, inserted obliquely, alternately disposed, averaging 14.1 pairs per 100 mm in length (550 mm)	50 pairs of nearly opposite polyp leaves, averaging 8 pairs per 100 mm in length (620 mm)
Distribution autozooids	Arranged in one row along the ventral edge of each developed polyp leaf (arrangement of gastrovascular cavities in the polyp leaves), but oriented alternately, appearing to be placed in two rows	Arranged in one row along the ventral edge of polyp leaves, sometimes crowdedly and alternately arranged so appear to be placed in two rows	Arranged in one row along the ventral edge of each developed polyp leaf (arrangement of gastrovascular cavities in the polyp leaves), but oriented alternately, appearing to be placed in two rows
Maximum number of autozooids per polyp leaf (colony size)	28 (952 mm)	26 (550 mm)	29 (620 mm)
Maximum size of the autozooids (length × width in mm)	4 × 1.5	4 × 2	4.1 × 1.7
Spiculate teeth in the autozooid's calyces	8, often of irregular development	up to 8	8, often of irregular development
Development of polyp leaves (colony size)	Narrow in lateral view, maximum length 40 mm, and dorsal edge slightly shorter than ventral edge, maximum width 6 mm (952 mm)	Deltoid in lateral view, with the bases 18 mm in maximum length, the ventral edges curved with maximum length 23 mm, and dorsal edges slightly shorter than ventral edges (550 mm)	Close to a right/obtuse triangle in lateral view, maximum length 50 mm, and dorsal edge slightly shorter than ventral edge maximum width 20 mm (620 mm)
Bases of polyp leaves overlapping	Yes	Yes	Yes
Distribution of mesozooids	On the dorsal side of rachis, in an elevated ridge of one or two lines, along the rachis and proximal dorsal edge of polyp leaves, up to 14 in number, decreasing in size from polyp leaf to dorsal track, the last ones of similar size to siphonozooids	On the dorsal side of rachis near the dorsal base of polyp leaves	On the dorsal side of rachis, in an elevated ridge of one or two lines, along the rachis and proximal dorsal edge of polyp leaves, up to 6 in number, decreasing in size from polyp leaf to dorsal track, the last ones of similar size to siphonozooids
Distribution of siphonozooids	Up to 0.26 mm in diameter, numerous, arranged in up to ~10 rows dorsally, running along the axillae of polyp leaves to the latero-dorsal sides of the rachis between polyp leaf insertions, resembling a "check mark" where the long stroke is placed between consecutive polyp leaves	0.2 mm in height and 0.3 mm in width, mostly conical with converging sclerites forming a pointed apex; arranged in 1–10 rows along the axillae of polyp leaves to the latero-dorsal sides of the rachis between polyp leaves	Up to 0.3 mm in diameter, numerous, arranged in up to ~6–8 rows dorsally, rows along the axillae of polyp leaves to the latero-dorsal sides of the rachis between polyp leaf insertions, resembling a "check mark". The line of siphonozooids running between consecutive polyp leaves can appear on the ventral track
Cross section of axis	Circular	Circular	Circular
Sclerites along the aboral side of tentacular axis	Three-flanged needles, up to 0.21 mm in length	Three-flanged needles, approximately up to 0.18 mm in length	Absent
Sclerites of the autozooids' calyces and teeth	Calyces: three-flanged needles, up to 0.59 mm in length. Teeth: three-flanged needles, up to	Calyces: three-flanged needles, up to 0.73 mm in length. Teeth: three-flanged needles, up to	Calyces: three-flanged needles, up to 0.8 mm in length. Teeth: three-flanged needles, up to

Table 2 (continued)

Characters / species	A. *moseleyi* comb. nov.[1,3]	A. *splendida*[2]	A. *williamsi* sp. nov.[3]
	0.97 mm in length	1.2 mm in length	1.2 mm in length
Sclerites of autozooids' pharynx	Three-flanged needles, up to 0.06 mm in length	Small three-flanged needles, up to 0.054 mm in length	Three-flanged needles, up to 0.06 mm in length
Sclerites of polyp leaves	Three-flanged needles, up to 1.1 mm in length	Three-flanged needles, up to 0.67 mm in length	Three-flanged needles, up to 0.75 mm in length
Sclerites of mesozooids	Three-flanged needles, up to 1.0 mm in length	Approximately up to 0.5 mm in length	Three-flanged needles, up to 0.95 mm in length
Sclerites of siphonozooid areas	Three-flanged needles, up to 0.9 mm in length	Three-flanged needles, up to 0.64 mm in length	Three-flanged needles, up to 0.57 mm in length
Sclerites of mid-rachis (dorsal tracks)	Three-flanged needles, up to 0.38 mm mid-dorsal track	n.d.	Three-flanged needles, up to 0.13 mm mid-dorsal track
Sclerites of lowermost part of rachis, above rachis-peduncle limit	Three-flanged needles, up to 0.37 mm at the lowest part	n.d.	Three-flanged needles, up to 0.14 mm at the lowest part, more robust (wider) than upper part (see Fig. 9 D and E comparatively)
Sclerites of peduncle	Short three-flanged rods up to 0.2 mm in length (slightly shorter at mid-length), some crosses up to 0.15 mm in length, more abundant at the mid and basal parts (where they can be 5 or 6 radiated), and minute bodies ~0.02 mm in length, also more abundant at basal end	Short three-flanged rods, up to 0.08 mm in length	Short three-flanged rods (sometimes pointed, flanges mainly noticeable at the ends, often simply as slits) up to 0.06 mm in length (of similar size at mid length), Y-shaped sclerites, crosses up to 0.055 mm in length, are present, and become more abundant and even, and 5 or 6-radiated at the middle parts. Minute bodies ~0.02 mm in length, also more abundant at basal end, where rods become rare
Colour of sclerites	All rachis, polyp leaves, and polyp sclerites are red. Peduncle with light red to transparent sclerites	Autozooids with needles from calycular teeth and upper part calyces yellow. Needles from tentacles, basal part of calyces, polyp leaves, siphonozooids, and rachis reddish. Mesozooids with yellowish sclerites. Rods from peduncle translucent to whitish	Autozooids with needles from calycular teeth and upper part of calyces yellow. Needles from basal part calyces, polyp leaves, siphonozooids, and rachis reddish. Mesozooids with yellowish sclerites. Rods and crosses from peduncle reddish to translucent
Development of lowermost polyp leaves	Decrease gradually in size, without any distinct zone of under-developed polyp leaves	Lowest seven pairs rudimentary	Decrease gradually in size, without any distinct zone of under-developed polyp leaves
Rachis-peduncle limit	With a moderate thickening	With a distinct swelling that forms an edged ring at the widest point	With a moderate thickening (single available colony damaged at this part)
Geographical and bathymetric distribution	Tasman Sea (off Sydney and central areas), 748 to ~1737 m in depth	Seamount Y3 near the Yap Trench in the Tropical Western Pacific, 879 m in depth	Puerto Rico, Caribbean Sea (NW Atlantic), 559 m in depth

sequenced. Both obtained sequences were in agreement with the previously published ones.

Alloptilella is identifiable as a monophyletic genus, being the sister group of all sequences of another distinct morphological and molecular genus recently revisited, the genus *Scytalium* (see Li et al. 2021; López-González 2021). The resurrection of the genus *Ptilella* (see García-Cárdenas et al. 2019) and the description of the genus *Alloptilella* resolve the polyphyletic situation of *Pennatula* observed in recent phylogenetic studies focused on the order Pennatulacea (e.g. Dolan et al. 2013; Kushida and Reimer 2018; García-Cárdenas et al. 2020). The realignment of *Pennatula* species in three different genera (based on molecular and morphological features) does not resolve the fact that the numerous named species of *Pennatula* are still in need of revision. Attending to the relatively high numbers of proposed species and the potential number of species recognizable as valid nowadays (Williams 1995, 2011), this is a task to be carried out in the future with the help of all available taxonomic tools. Molecular information seems to be essential in that revision, or at least the re-description of the already supposedly well-known species, such as *Pennatula phosphorea* Linnaeus, 1758, *P. aculeata* Danielssen, 1860, and *P. rubra* (Ellis, 1764), among others (see García-Cárdenas et al. 2019).

The description of the genus *Alloptilella* was based on *Alloptilella splendida*, a species inhabiting seamounts in the Tropical Western Pacific at up to 879 m depth. The erection of a new *Pennatula*-like genus from a molecular point of view was completely necessary. This species is morphologically and chromatically close to *Pennatula naresi* Kölliker, 1880 (see Kölliker 1880: 5, Plt. I, Figs, 1, 2). García-Cárdenas et al. (2019) suggested that the latter species could belong to the genus *Ptilella*, but more morphological and molecular studies were necessary. The original description of *P. naresi* included enough details on the distribution and colour of the sclerites in the autozooids, mesozooids (named ventral zooids), and siphonozooids (named lateral zooids). The gastrovascular cavities of autozooids are arranged in the polyp leaves in a single line, and the yellow calyces are oriented in alternate directions giving the impression of being arranged in two series. The mesozooids, armed with yellow sclerites, form a row of polyps decreasing in size "which begin at the ventral margin of the pinnule at a little distance from its attachment, run obliquely upon the sides of the rachis, and end with a longitudinal streak". The siphonozooids occupy the space between mesozooid rows also running between consecutive polyp leaves. Kölliker (1880) stated that only autozooids and mesozooids (as ventral zooids) are armed with yellow sclerites, as *A. splendida*. Li et al. (2021) mainly differentiate *A. splendida* and *P. naresi* in the placement of mesozooids, restricted to the dorsal area in *A. splendida* and also occupying the proximalmost part of the polyp leaf edge dorsally. The taxonomic placement of *P. naresi* is controversial from a

morphological point of view. The arrangements of autozooids, mesozooids, and siphonozooids agree with *Alloptilella*; hence, a complete morphological redescription of its type material is desirable.

Identification by DNA sequencing of the three morphologically similar genera is well established, although molecular differentiations among the three *Alloptilella* species are low. The *mtMutS* sequences of the Caribbean (*A. williamsi* sp. nov.) and Tasman (*A. moseleyi* comb. nov.) species are identical, while *A. splendida* (Tropical Western Pacific) differs in a single base. The *ND2* sequences of *A. williamsi* sp. nov. and *A. moseleyi* comb. nov. (not available for *A. splendida*) differ also in a single base. The *COI* sequences of *A. splendida* and *A. williamsi* sp. nov. differ in two bases (only 539 bases are known for *A. splendida*). Remarkably, the nuclear *28S* differs in a single base between *A. splendida* (Tropical Western Pacific) and *A. williamsi* sp. nov. (Caribbean Sea) (only 677 bases are known for *A. splendida*), while no information is currently available for *A. moseleyi* comb. nov.

A similar situation occurs among the three species of *Ptilella* (*P. grandis*, *P. grayi*, and *P. inflata*) (see Table 2, Fig. 12, SMFigs. 1, 2 in this paper and García-Cárdenas et al. 2019). For this paper, two mitochondrial (*mtMutS* and *ND2*) segments and one nuclear (*28S*) segment from SW Atlantic specimens of *Ptilella inflata* have been sequenced. *Ptilella grandis* and *P. inflata* share an identical sequence of *mtMutS*, while *P. grayi* shows differences in two bases. *ND2* sequences of *P. grandis* differ in four bases with *P. grayi*, but only in two with *P. inflata*, while *P. grayi* and *P. inflata* differ also in two bases. Two bases differentiate *P. grandis* and *P. grayi* *COI* sequences (not available for *P. inflata*). Surprisingly, differences in the nuclear *28S* are also low, *P. grayi* differs in three bases with *P. grandis*, and in four bases with *P. inflata*, while *P. grandis* and *P. inflata* only differ in a single base.

From a chromatic point of view, *Alloptilella splendida* and *A. williamsi* sp. nov. share the same distribution pattern of coloured sclerites. Autozooids and mesozooids have yellow sclerites, while the rest of the sclerites in the colony are red, being light red or translucent in the lower parts of the peduncle. In the case of *A. moseleyi*, sclerites in all parts of the rachis are red, having a similar colour pattern in the peduncular sclerites to its congeners. However, *A. splendida* and *A. moseleyi* have red three-flanged sclerites along the aboral side of the tentacles, while in *A. williamsi* sp. nov. tentacular sclerites are completely absent.

From a morphological point of view (apart from the above-mentioned chromatic differences), both western Pacific species (*Allopilella moseleyi* and *A. splendida*) have a similar appearance (see Table 2 for a complete comparative overview). The polyp leaves seem to be placed in a more opposite than alternate arrangement in *A. moseleyi*. Polyp leaves seem to be narrowest and proportionally longer in

A. moseleyi than those in *A. splendida.* Differences in the number of polyp leaves (126 vs. 65 may be due to the different sizes of the available colonies), with *A. moseleyi* also having a slightly higher density of polyp leaves per 100 mm of rachis (18 vs. 14.1). Tentacular sclerites are slightly shorter in *A. moseleyi* (up to 0.18 vs. 0.21 mm), but sclerites from polyp leaves, mesozooids, siphonozooids, and peduncle are larger in *A. moseleyi* (Table 2). Finally, the lowest pairs of polyp leaves decrease gradually in size in *A. moseleyi* without any distinct zone of under-developed polyp leaves as occurs in *A. splendida*.

The new proposed species, *Alloptilella williamsi* sp. nov., is from a chromatic point of view, close to the type species of the genus, *A. splendida*. However, the new species differs in an opposite disposition of polyp leaves, absence of sclerites in the tentacles, a reduced number of polyp leaves per 100 mm of rachis (8 vs. 14.1), larger polyp leaves (in preserved state), presence of 1–2 mesozooids on the proximal dorsal edge of polyp leaves, larger sclerites in mesozooids (0.95 vs. 0.5 mm), and peduncle three-flanged rods of different shape (Li et al. 2021: Fig. 2f and Fig. 10a, c of this paper), as well as additional type sclerites (Y-shaped, crosses, 5–6 radiates twinning) in the peduncle (minute bodies are common in the peduncle of sea pens, perhaps a detailed search in the holotype of *A. splendida* could discover also this type, so I will not use this feature in this comparison), and a different developmental pattern in the lowermost polyp leaves (Table 2).

Despite the above-listed chromatic and morphological differences between the three *Alloptilella* species, they are very close from a molecular view (as occurs also between *Ptilella* species), at least when we compare the traditional markers used, the mitochondrial *mtMutS*, *ND2*, *COI*, and even the nuclear *28S*. These differences have been detailed above, but in summary, they can be one or two bases per marker, and sometimes none (e.g. *mtMuts* sequences of the Tasman Sea *A. moseleyi* comb. nov. and the Caribbean *A. williamsi* sp. nov.). It is true that the molecular coverage of the four markers used is not complete for all species, but it seems also that, at least in *Alloptilella* (and also *Ptilella*), additional and more variable molecular markers (such as the nuclear ITS region, and SRP54, see Aguilar and Sánchez 2007; Grajales et al. 2007; Concepcion et al. 2008) should also be explored in the future. In the case of *Alloptilella* (and *Ptilella*), we are close to that percentage of cases (~ 25–30%) in which the considered most variable molecular marker in octocorals (*mtMutS*) provides little or no information (McFadden et al. 2014).

García-Cárdenas et al. (2019) proposed the assignation of *Pennatula bellissima* Fowler, 1888, to the genus *Ptilella*, as well as the possible synonymy of *Pennatula bayeri* Castro & Medeiros, 2001, but also suggested that a molecular characterization of this species is needed, because the alternate orientation of autozooids along the ventral edge of polyp leaves is not in agreement with the autozooid's arrangement of *Ptilella grandis* and other *Ptilella* species also discussed in this paper. However, the distribution of mesozooids in *P. bellissima* agrees with that described for *Ptilella* species. On the other hand, the presence of one or two mesozooids on the proximal dorsal edge of polyp leaves in *Pennatula rubra* (Ellis, 1764) (see Kükenthal 1915; Altuna 2015; García-Cárdenas et al. 2019) resembles a feature present in *Alloptilella*. However, *P. rubra* does not present additional mesozooid polyps forming a ridge along the dorsal side of the rachis directed upwardly.

Under the current typological criteria in the description of new species, and considering the importance of molecular knowledge in the differentiation of the species in some of pennatulacean genera, such as the three similar genera *Pennatula*, *Ptilella*, and *Alloptilella*, the development of economically viable ancient DNA molecular techniques would help in the complementary molecular characterization of the old preserved type material. This should be carried out with the necessary agreement and acceptance for tissue sampling by the major museums that house ancient collections such as the NHM in London, the MNHN in Paris, Naturalis Biodiversity Center in Leiden, and the National Museum of Natural History (Smithsonian Institution) in Washington, among others. Successful molecular exploration of old type materials will surely avoid continual hypothesis building and will reduce discussions when morphological features sometimes overlap or are controversial due to poor knowledge of inter- and intraspecific variability. The set of ancient types of *Pennatula* species described by Kölliker would be a perfect target for the application of the aforementioned molecular techniques, helping to achieve a final generic assignment and the molecular characterization of the species.

Declarations

References

Aguilar C, Sánchez JA (2007) Phylogenetic hypotheses of gorgoniid octocorals according to ITS2 and their predicted RNA secondary structures. Mol Phylogenet Evol 43:774–786. https://doi.org/10.1016/j.ympev.2006.11.005

Alfaro ME, Zoller S, Lutzoni F (2003) Bayes or Bootstrap? A simulation study comparing the performance of Bayesian Markov chain Monte Carlo sampling and bootstrapping in assessing phylogenetic confidence. Mol Biol Evol 20:255–226. https://doi.org/10.1093/molbev/msg028

Altuna A (2015) Identificación de las especies ibéricas del género *Pennatula* L., 1758 (Octocorallia: Pennatulacea). Campañas Demersales, Ecomarg, Indemares y Medits. Insub:11

Bayer FM, Stefani J (1988) Primnoidae (Gorgonacea) de Nouvelle-Caledonie. Bull Mus Natl Hist Nat 10(A)3:449–476

Bayer FM, Grasshoff M, Verseveldt J (1983) Illustrated trilingual glossary of morphological and anatomical terms applied to Octocorallia. Brill/ Backhuys, Leiden

Castro CB, Medeiros MS (2001) Brazilian Pennatulacea (Cnidaria: Octocorallia). Bull Biol Soc Wash 10:140–159

Concepcion GT, Crepeau MW, Wagner D, Kahng SE, Toonen RJ (2008) An alternative to ITS, a hypervariable, single-copy nuclear intron in corals, and its use in detecting cryptic species within the octocoral genus *Carijoa*. Coral Reefs 27:323–336. https://doi.org/10.1007/s00338-007-0323-x

Danielssen DC (1860) Beskrivelse over en ny Art *Virgularia*. Forhandl Videnskabs-selsk Christiania. 1859:251

Dolan E, Tyler PA, Yesson C, Rogers AD (2013) Phylogeny and systematics of deep-sea sea pens (Anthozoa: Octocorallia: Pennatulacea). Mol Phylogenet Evol 69(3):610–618. https://doi.org/10.1016/j.ympev.2013.07.018

Ehrenberg CG (1834) Beitrage zur physiologishcen Kenntniss der Corallenthiere im allgemeinen, und besonders des rothen Meeres, nebst einem Versuche zur physiologischen Systematik derselben. Abh Königl Akad Wiss Berlin 1832:225–380

Ellis J (1764) An account of the sea pen, or *Pennatula phosphorea* of Linnaeus; likewise a description of a new species of sea pen, found on the coast of South-Carolina, with observations on sea-pens in general. In a letter to the honourable Coote Molesworth, Esq.; M.D. and F.R.S. from John Ellis, Esq; F.R.S. and member of the Royal Academy of Upsal. Philos T R Soc Lon 53:419–435

France SC, Hoover LL (2002) DNA sequences of the mitochondrial COI gene have low levels of divergence among deep-sea octocorals (Cnidaria: Anthozoa). Hydrobiologia 471:149–155. https://doi.org/10.1023/A:1016517724749

Fowler GH (1888) On a new Pennatula from the Bahamas. Proc Zool Soc Lond 1888: 135–140

García-Cárdenas FJ, Drewery J, López-González PJ (2019) Resurrection of the sea pen genus *Ptilella* Gray, 1870 and description of *Ptilella grayi* n. sp. from the NE Atlantic (Octocorallia: Pennatulacea). Sci Mar 83(3):261–276. https://doi.org/10.3989/scimar.04845.26A

García-Cárdenas FJ, Núñez-Flores M, López-González PJ (2020) Molecular phylogeny and divergence time estimates in pennatulaceans (Cnidaria: Octocorallia: Pennatulacea). Sci Mar 84: 317–330. https://doi.org/10.3989/scimar.05067.28A

Grajales A, Aguilar C, Sánchez JA (2007) Phylogenetic reconstruction using secondary structures of Internal Transcribed Spacer 2 (ITS2, rDNA): finding the molecular and morphological gap in Caribbean gorgonian corals. BMC Evol Biol 7:90. https://doi.org/10.1186/1471-2148-7-90

Gray JE (1870) Catalogue of sea-pens or Pennatulariidae in the collection of the British Museum. London. https://doi.org/10.5962/bhl.title.11307

Haeckel E (1866) Generelle Morphologie der organismen. Georg Reimer, Berlin

Herklots JA (1858) Notices pour servir à l'étude des polypiers nageurs ou pennatulidés. Bijdr Dierkd 7:1–31

Hickson SJ (1916) The Pennatulacea of the Siboga Expedition, with a general survey of the order. Siboga Exped Monogr 14(77):1–265

Hillis DM, Bull JJ (1993) An empirical test of bootstrapping as a method for assessing confidence in phylogenetic analysis. Syst Biol 42:182–192. https://doi.org/10.1093/sysbio/42.2.182

Huelsenbeck JP, Ronquist F (2001) MrBAYES: Bayesian inference of phylogenetic trees. Bioinformatics 17:754–755. https://doi.org/10.1093/bioinformatics/17.8.754

Kimura M (1980) A simple method for estimating evolutionary rates of base substitutions through comparative studies of nucleotide-sequences. J Mol Evol 16(2):111–120

Kölliker RA (1880) Report on the Pennatulida dredged by H. M. S. Challenger during the years 1873-1876. Rep Sci Res Voy HMS Challenger 1873-76. Zoology 1(2):1–41

Kükenthal W (1910) Pennatuliden der Deutschen Tiefsee-Expedition. Zool Anz 36(2/3):51–58

Kükenthal W (1915) Pennatularia. Das Tierreich. Verlag von R, Friedländer und Sohn, Berlin

Kushida Y, Reimer JD (2018) Molecular phylogeny and diversity of sea pens (Cnidaria: Octocorallia: Pennatulacea) with a focus on shallow water species of the northwestern Pacific Ocean. Mol Phylogenet Evol 131:233–244. https://doi.org/10.1016/j.ympev.2018.10.032

Lamouroux JVF (1812) Extrait d'un memoire sur la classification des polypiers coralligenes non entierement pierreux. Nouv Bull Sci Soc Philomatique Paris 3(63):18l–188l

Li Y, Zhan Z, Xu K (2020) Morphology and molecular phylogenetic analysis of deep-sea purple gorgonians (Octocorallia: Victorgorgiidae) from seamounts in the tropical western pacific, with description of three new species. Front Mar Sci 7:701. https://doi.org/10.3389/fmars.2020.00701

Li Y, Zhan Z, Xu K (2021) Establishment of *Alloptilella splendida* gen. et sp. nov. and resurrection of *Scytalium veneris* (Thomson & Henderson, 1906), two sea pens (Cnidaria: Pennatulacea) from seamounts in the tropical Western Pacific. J Oceanol Limnol 39(5):1790–1804. https://doi.org/10.1007/s00343-021-1083-0

Linnaeus C (1758) Systema naturae. Editio decima, reformata, Holmiae

López-González PJ (2020) A new calcaxonian genus and family for *Trichogorgia utinomii* Cordeiro, 2019 (Octocorallia, Alcyonacea): new recordsof a scleriteless gorgonian species from Antarctica. Mar Biodivers 50:96. https://doi.org/10.1007/s12526-020-01109-0

López-González PJ (2021) *Scytalium herklotsi* sp. nov. (Anthozoa, Octocorallia, Pennatulacea), the first Atlantic species in the genus *Scytalium* Herklots, 1858. Mar Biodivers 51:62. https://doi.org/10.1007/s12526-021-01200-0

López-González PJ, Drewery J (2022) When distant relatives look too alike: a new family, two new genera and a new species of deep-sea *Umbellula*-like sea pens (Anthozoa, Octocorallia, Pennatulacea). Invertebr Syst 36, 199–225. https://doi.org/10.1071/IS21040

López-González PJ, Gili J-M, Williams GC (2001) New records of Pennatulacea (Anthozoa: Octocorallia) from the African coast, with description of a new species and a zoogeographic analysis. Sci Mar 65(1):59–74

McFadden CS, van Ofwegen LP (2013) A second, cryptic species of the soft coral genus *Incrustatus* (Anthozoa: Octocorallia: Clavulariidae) from Tierra del Fuego, Argentina revealed by DNA barcoding. Helgol Mar Res 67:137–147. https://doi.org/10.1007/s10152-012-0310-7

McFadden CS, van Ofwegen LP (2013) Molecular phylogenetic evidence supports a new family of octocorals and a new genus of Alcyoniidae (Octocorallia, Alcyonacea). Zookeys 346: 59-83. https://doi.org/10.3897/zookeys.346.6270

McFadden CS, Tullis ID, Hutchinson MB et al (2004) Variation in coding (NADH dehydrogenase subunits 2, 3, and 6) and noncoding intergenic spacer regions of the mitochondrial genome in Octocorallia (Cnidaria: Anthozoa). Mar Biotechnol 6:516–526. https://doi.org/10.1007/s10126-002-0102-1

McFadden CS, Brown AS, Brayton C, Hunt CB, van Ofwegen LP (2014) Application of DNA barcoding in biodiversity studies of shallow water octocorals: molecular proxies agree with morphological estimates of species richness in Palau. Coral Reefs 33:275–286. https://doi.org/10.1007/s00338-013-1123-0

Pante E, France SC (2010) *Pseudochrysogorgia bellona* n. gen. n. sp.: a new genus and species of chrysogorgiid octocoral (Coelenterata: Anthozoa) from the Coral Sea. Zoosystema 32:595–612 https://doi.org/10.5252/z2010n4a4

Pante E, France SC, Couloux A, Cruaud C, McFadden CS, Samadi S, Watling L (2012) Deep-sea origin and in-situ diversification of chrysogorgiid octocorals. PLoS ONE 7(6):E38357. https://doi.org/10.1371/journal.pone.0038357

Rambaut A, Drummond AJ, Xie D, Baele G, Suchard MA (2018) Posterior summarization in Bayesian phylogenetics using Tracer 1.7. Syst Biol 67:901–904. https://doi.org/10.1093/sysbio/syy032

Ronquist F, Huelsenbeck JP (2003) MrBayes 3: Bayesian phylogenetic inference under mixed models. Bioinformatics 19(12):1572–1574

Sánchez J, McFadden CS, France S, Lasker H (2003) Molecular phylogenetic analyses of shallow-water Caribbean octocorals. Mar Biol 142:975–987. https://doi.org/10.1007/s00227-003-1018-7

Saucier EH, France SC, Watling L (2021) Toward a revision of the bamboo corals: part 3, deconstructing the family Isididae. Zootaxa 504(3):247–272. https://doi.org/10.11646/zootaxa.5047.3.2

Tamura K, Stecher G, Peterson D, Filipski A, Kumar S (2013) MEGA6: Molecular Evolutionary Genetics Analysis Version 6.0. Mol Biol Evol 30:2725–2729. https://doi.org/10.1093/molbev/mst197

Verrill AE (1865) Synopsis of the polyps and corals of the North Pacific Exploring Expedition, under Commodore C. Ringgold and Captain John Rogers, U.S.N., from 1853 to 1856. Collected by Dr. W. Stimpson, naturalist of the Expedition. With descriptions of some additional species from the west coast of North America. Proc Essex Inst 4:181–196

Wagner D, Sowers D, Williams SM, Auscavitch S, Blaney D, Cromwell M (2019) EX-18-11 Expedition Report - Océano Profundo 2018: exploring deep-sea habitats off Puerto Rico and the U.S. Virgin Islands. NOAA, Silver Spring. https://doi.org/10.25923/wc2n-qg29

Williams GC (1995) Living genera of sea pens (Coelenterata: Octocorallia: Pennatulacea): illustrated key and synopses. Zool J Linnean Soc 113:93–140. https://doi.org/10.1006/zjls.1995.0004

Williams GC (2011) The global diversity of sea pens (Cnidaria: Octocorallia: Pennatulacea). PLoS One 6:e22747. https://doi.org/10.1371/journal.pone.0022747